Search for electroweak-scale dijet resonances using trigger-level analysis with the ATLAS detector in 132 fb^{-1} of pp collisions at $\sqrt{s}=13$ TeV

G. Aad *et al.*[*]
(ATLAS Collaboration)

(Received 3 September 2025; accepted 14 October 2025; published 24 November 2025)

This article reports on a search for dijet resonances using 132 fb^{-1} of pp collision data recorded at $\sqrt{s}=13$ TeV by the ATLAS detector at the Large Hadron Collider. The search is performed solely on jets reconstructed within the ATLAS trigger to overcome bandwidth limitations imposed on conventional single-jet triggers, which would otherwise reject data from decays of sub-TeV dijet resonances. Collision events with two jets satisfying transverse momentum thresholds of $p_{\mathrm{T}} \geq 85$ GeV and jet rapidity separation of $|y^{*}| < 0.6$ are analysed for dijet resonances with invariant masses from 375 to 1800 GeV. A data-driven background estimate is used to model the dijet mass distribution from multijet processes. No significant excess above the expected background is observed. Upper limits are set at 95% confidence level on coupling values for a benchmark leptophobic axial-vector Z' model and on the production cross section for a new resonance contributing a Gaussian-distributed line-shape to the dijet mass distribution.

DOI: 10.1103/15p2-bkg8

I. INTRODUCTION

A key strength of collider experiments is their ability to discover new particles and observe their properties. This capability has led to many of the major discoveries of particle physics in the last four decades, notably that of the $W^{\pm}$ and Z bosons [1–4], top quark [5,6], and the Higgs boson [7,8] in the mass range 81 to 173 GeV, around what is known as the "electroweak scale." Nevertheless, the electroweak scale remains to be fully explored.

The ATLAS experiment [9] at the Large Hadron Collider (LHC) [10] is one of two experiments where the Higgs boson was discovered with approximately 11 fb^{-1} of pp collision data. ATLAS recorded a factor of ~13 times more data during Run 2 (2015–2018), providing an unprecedented data sample to search for evidence of additional particles with masses at and above the electroweak scale. Dijet resonances constitute a primary search signature for new particles. For example, any mediator particle capable of being produced directly in pp collisions should be able to decay into a dijet signature. Searches for dijet resonances, however, have been impeded by the large background from multijet processes in the Standard Model (SM), which are produced with rates that overwhelm the normal data-taking capabilities of the ATLAS and CMS [11] detectors. Consequently, it has been difficult for LHC searches to constrain electroweak-scale dijet resonances with the same coupling sensitivity as at multi-TeV masses.

Both ATLAS and CMS have targeted sub-TeV masses with new dijet searches using their large samples of Run-2 collisions. In 2018, ATLAS published a search for dijet resonances using an innovative technique, trigger-level analysis (TLA), on one quarter of that sample [12]. The TLA technique overcomes the normal data-taking limitations by recording the data as reconstructed and reduced by the ATLAS trigger system, rather than the full detector data stream, for subsequent analysis. With much greater statistical power than available in traditional data-taking, the TLA technique allowed ATLAS to constrain dijet resonances at masses from 450 to 1800 GeV, far below the minimum mass of 1.5 TeV probed by the conventional ATLAS dijet searches in Run 2 [13]. A similar technique to TLA ("data scouting") was prototyped by CMS with data at 7 TeV center-of-mass energy and employed in CMS dijet analyses, constraining resonances in the mass range 500 to 1800 GeV [14–16]. Similarly, LHCb [17] employs the "turbo stream" as one of their main data-taking strategies [18,19]. Searches for dijet resonances in complementary channels were performed with additional requirements on the dijet system, such as large transverse momentum (p_{T}) [20,21], photon or jet initial-state radiation [20,22,23], an additional charged lepton [24], or b-tagging of the jets [13,16,21,25–27] by ATLAS and CMS. These searches allowed ATLAS to cover a wider region of dijet mass from 100 GeV up to multiple TeV than previous searches by

---

[*] Full author list given at the end of the article.

ATLAS, albeit with limited acceptance due to the additional requirements and, consequently, less sensitivity than the TLA result.

This paper presents an updated TLA search for dijet resonances in the mass range 375 to 1800 GeV using the full statistical power of the sample recorded by ATLAS during Run 2. Superseding the prior ATLAS TLA result [12], this new search incorporates four times the integrated luminosity, an improved first-level trigger strategy to extend the search to lower dijet masses, an improved jet calibration, and more sophisticated statistical analysis techniques.

II. ATLAS DETECTOR

The ATLAS detector [9] at the LHC covers nearly the entire solid angle around the collision point.[1] It consists of an inner tracking detector surrounded by a thin superconducting solenoid, electromagnetic and hadron calorimeters, and a muon spectrometer incorporating three large superconducting air-core toroidal magnets. The inner-detector system (ID) is in a 2 T axial magnetic field and provides charged-particle tracking in the range $|\eta| < 2.5$. The high-granularity silicon pixel detector covers the vertex region and typically provides four measurements per track, the first hit normally being in the insertable B-layer (IBL) installed before Run 2 [28,29]. It is followed by the silicon microstrip tracker (SCT), which usually provides eight measurements per track. These silicon detectors are complemented by the transition radiation tracker (TRT), which enables radially extended track reconstruction up to $|\eta| = 2.0$. The TRT also provides electron identification information based on the fraction of hits (typically 30 in total) above a higher energy-deposit threshold corresponding to transition radiation.

The calorimeter system covers the pseudorapidity range $|\eta| < 4.9$. Within the region $|\eta| < 3.2$, electromagnetic calorimetry is provided by barrel and end cap high-granularity lead/liquid-argon (LAr) calorimeters, with an additional thin LAr presampler covering $|\eta| < 1.8$ to correct for energy loss in material upstream of the calorimeters. Hadron calorimetry is provided by the steel/scintillator-tile calorimeter, segmented into three barrel structures within $|\eta| < 1.7$, and two copper/LAr hadron end cap calorimeters. The solid angle coverage is completed with forward copper/LAr and tungsten/LAr calorimeter modules optimised for electromagnetic and hadronic energy measurements respectively.

The muon spectrometer comprises separate trigger and high-precision tracking chambers measuring the deflection of muons in a magnetic field generated by the superconducting air-core toroidal magnets.

Collision events of interest are selected by a first-level (L1) trigger system implemented in custom hardware, followed by selections made by algorithms implemented in software in a high-level trigger (HLT) [30]. The L1 trigger accepts events from the 40 MHz bunch crossings at a rate below 100 kHz and features a topological processor, L1Topo [31], allowing selections on multibody quantities such as the angular distance between two jets. The HLT reconstructs events accepted by the L1 to record an average of 1.2 kHz of full events with an average size of 1 MB to permanent storage in a “main” stream [32]. Specialized streams record additional data for low-p_{T} flavor physics analysis, monitoring, calibration, and other uses. These streams use dedicated triggers, non-standard reconstruction paths, or readout of only subsets of the detector around regions of interest. For TLA, a dedicated stream stores the HLT jet information [30,33] for all events accepted by certain L1 trigger selections, regardless of the HLT decision, while discarding the raw detector data found in the main stream. The information recorded for each HLT jet consisted of the four-momentum and calorimeter variables providing information about the quality and structure of each jet [34]. No tracking measurements were recorded for TLA. The TLA stream recorded events with a rate of up to 27 kHz at a mean 6.5 kB per event [32]. An extensive software suite [35] is used in the detector operations, trigger and data acquisition systems of the experiment, and in simulation, reconstruction, and analysis.

III. DATA AND SIMULATION SAMPLES

Data were selected by several L1 triggers and processed by the TLA stream for offline analysis as follows. In each collision, the L1 trigger identified L1 jets from $\Delta\eta \times \Delta\phi = 0.2 \times 0.2$ electromagnetic and hadronic calorimeter segments with a sliding-window algorithm. Events containing at least one L1 jet within $|\eta| < 3.1$ with sufficient transverse momentum were recorded in the TLA stream. From 2016–2018, this requirement was $p_{\mathrm{T}} > 100$ GeV, which corresponds to the lowest-threshold, unprescaled single-jet L1 trigger for most of that period. Starting in 2017, additional prescaled triggers with lower thresholds were included at the end of LHC fills as declining instantaneous luminosity during a fill lowered the actual trigger rate of the initial L1 menu well below its capability, yielding a peak rate of 27 kHz. In 2017, a single end-of-fill trigger required an L1 jet with $p_{\mathrm{T}} > 50$ GeV. In 2018, this was expanded to a luminosity-dependent combination of triggers, from which events were selected for analysis with either of two triggers. The first required a single L1 jet with $p_{\mathrm{T}} > 50$ GeV. The second, making use of the L1Topo processor, required two L1 jets satisfying $p_{\mathrm{T}} > 50$ GeV for the leading jet,

---

[1] ATLAS uses a right-handed coordinate system with its origin at the nominal interaction point (IP) in the centre of the detector and the z-axis along the beam pipe. The x-axis points from the IP to the centre of the LHC ring, and the y-axis points upwards. Cylindrical coordinates (r, ϕ) are used in the transverse plane, ϕ being the azimuthal angle around the z-axis. The pseudorapidity is defined in terms of the polar angle θ as $\eta = -\ln\tan(\theta/2)$. Angular distance is measured in units of $\Delta R \equiv \sqrt{(\Delta\eta)^2 + (\Delta\phi)^2}$.

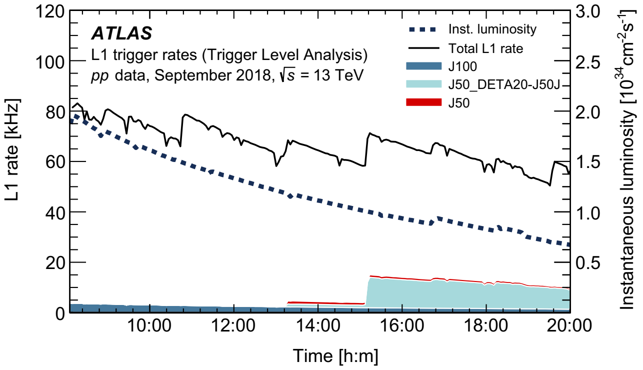

FIG. 1. Trigger rate as a function of time for the total L1 trigger and the L1 triggers feeding the TLA stream. The single LHC fill shown occurred in September 2018. While the J100 L1 item (dark blue histogram) collected events for TLA throughout the fill, the single-jet J50 and dijet J50_DETA20-J50J triggers (light blue and red histograms) activated as the LHC instantaneous luminosity (dashed line) and total L1 trigger rate (solid line) declined during the fill.

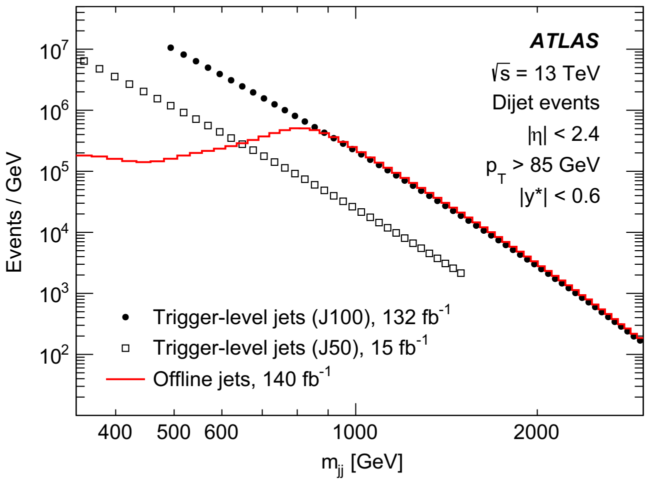

FIG. 2. Distributions of dijet invariant mass m_{jj} for events collected via the TLA stream and reconstructed in the HLT, combining events selected at L1 by the $p_{\mathrm{T}} > 100$ GeV trigger (filled circles) and the prescaled single-jet and dijet $p_{\mathrm{T}} > 50$ GeV triggers (open squares), showing the increase in events recorded at lower values of dijet mass for this analysis compared with events collected via the main stream and reconstructed offline (histogram). For this illustrative comparison, each sample must satisfy the analysis selection described in Sec. V, except for rejection of the tile gap region, and includes events with at least two trigger or offline jets, each with $p_{\mathrm{T}} > 85$ GeV and $|\eta| < 2.4$, with half a rapidity difference smaller than 0.6. The final sample used for the search is discussed and shown separately in Sec. V.

$p_{\mathrm{T}} > 15$ GeV for the subleading jet, and $|y^*| < 1$, where $|y^*| \equiv |\Delta\eta/2|$ is half of the absolute rapidity difference between the two jets. No data recorded in 2015 are considered, as only a small amount of luminosity was recorded with the TLA stream that year, requiring an L1 jet with $p_{\mathrm{T}} > 75$ GeV. That sample is fully analysed in the prior ATLAS dijet TLA [12]. Figure 1 shows the typical rate for the individual TLA streams during an LHC fill.

In addition to the data used for the search, collision events recorded with the main stream and reconstructed offline were used to calibrate the jets used for the search and to validate the statistical methods applied to the TLA stream. Events in the main stream provide a superset of the information available for events in the TLA stream and are thus suitable to derive a calibration for the latter. The two streams were triggered independently, with the decision to record an event in one stream unaffected by the decision to record an event in the other. The main stream was not used to construct the search sample. Main stream events were recorded with a suite of unprescaled and prescaled single-jet triggers with various p_{T} thresholds as low as 45 GeV. The unprescaled single-jet trigger with the lowest threshold required $p_{\mathrm{T}} > 420$ GeV at the HLT selection.

All data used from the TLA and main streams were recorded in stable beam conditions with all relevant detector systems operating normally [36]. Events are discarded if occurring during brief periods associated with calorimeter data corruption or transient LAr calorimeter noise [37]. The number of pp interactions per bunch crossing, referred to as pile-up, spanned 10–70 interactions per bunch crossing (μ), with an average of $\mu = 25$ in 2016, $\mu = 38$ in 2017, and $\mu = 36$ in 2018. Pile-up both from the same bunch crossing ("in-time") and preceding bunch crossings ("out-of-time") affects the energy reconstruction in the calorimeters and is corrected for in a dedicated step of the jet calibration.

After trigger and data-quality requirements, this search uses 132 fb^{-1} of data collected from 2016 to 2018 with the TLA stream via the $p_{\mathrm{T}} > 100$ GeV L1 trigger ("J100") and 15 fb^{-1} recorded with the $p_{\mathrm{T}} > 50$ GeV L1 end-of-fill single-jet and dijet triggers ("J50"). These two datasets overlap since J50-triggered events with a jet of sufficiently high p_{T} also fulfill the requirements of the unprescaled J100 trigger. Figure 2 compares the samples collected by the TLA and main streams as a function of dijet invariant mass.

Relative to the sample collected with the main stream using both prescaled and unprescaled triggers, the J50 TLA sample provides up to ∼30 times greater numbers of events per mass bin and the J100 TLA sample provides up to ∼75 times greater numbers of events.

Events from simulation of multijet processes are used to derive calibrations of jet energy measurements and evaluate the effects of certain systematic uncertainties, described below. These events were simulated with Pythia 8.235 [38], the A14 [39] set of tuned parameters for the underlying event, and the leading-order NNPDF2.3 [40] parton distribution functions (PDFs). The renormalization and factorisation scales were set to the average p_{T} of the two leading jets. In order to model the effect of pile-up, the hard-scatter event was overlaid with simulated minimum-bias events generated with Pythia 8.186 [41] using the leading-order NNPDF2.3 PDFs and the A3 set of tuned parameters [42]. The events were reweighted such that the resulting distribution of average number of interactions per bunch crossing matches that observed in data. Detector effects were simulated using Geant4 [43] within the ATLAS software infrastructure [35,44]. Separate samples were constructed for each year of data taking to reflect the changes in luminosity profile and detector conditions.

Additional spin-1 Z' bosons often arise in models of phenomena beyond the Standard Model (BSM), such as in those involving symmetry breaking of extended gauge theories, Kaluza-Klein towers arising from extra dimensions, and in many others. As a benchmark for these and other resonances, a leptophobic Z' model [45] was simulated at leading order, with matrix elements calculated in MadGraph 5 2.2.3 [46] using the leading-order NNPDF2.3 PDFs and parton showering performed in Pythia 8.210 with EvtGen 1.2.0 [47] and the A14 set of tuned parameters. Detector effects including the effects of pile-up were simulated as for the sample of multijet processes using the ATLAS simulation. The Z' model assumes axial-vector couplings to all SM quarks with one coupling value common to all quark flavor. The Z' simulation did not model interference with the SM, such as with the Z boson. The model includes a coupling of the Z' to a dark matter candidate, but the simulation adopted a scenario [45,48] where its decays into dark matter are negligible. In this case, the dijet production rate and resonance width depend, at leading order, only on the coupling to quarks, g_q, and the mass of the resonance, $m_{Z'}$. The production rate scales quadratically with g_q.

IV. JET RECONSTRUCTION AND CALIBRATION

Jets were reconstructed by the HLT ("trigger jets") solely from topological clusters of signals in contiguous calorimeter cells [49] using the anti-k_t algorithm [50,51] with a radius parameter of $R = 0.4$. Each cluster is assigned an energy equal to the sum of the associated cell energies. These signals are calibrated at the electromagnetic (EM) scale, accounting correctly for the energy deposited by EM showers but not by hadronic showers. Consequently, the resulting jets formed from such topological clusters (EMTopo) require further calibration. For this search, only trigger jets are available. The analysis discards jets with $p_{\mathrm{T}} < 85$ GeV or $|\eta| > 2.4$ to minimise the contribution of pile-up jets and to achieve the best possible jet resolution. Events that contain jets induced by calorimeter noise, beam-induced background, or cosmic rays were rejected using the "BadLoose" criteria identical to Ref. [34] but with no requirement on the track-based charged fraction, which was not recorded for trigger-level jets but has a negligible effect after the requirement on the rapidity difference described in Sec. V.

A calibration procedure was performed for trigger jets during the analysis to correct their energy and direction to those of particle-level jets. This calibration made use of two additional types of jet reconstruction. For main stream data, used in the final calibration step, an additional collection of jets was reconstructed from the raw detector data ("offline jets") with an equivalent anti-k_t $R = 0.4$ algorithm and kinematic selections, calibrated using the standard ATLAS techniques [52]. For simulated data, anti-k_t $R = 0.4$ particle-level jets were reconstructed from stable particles with a lifetime greater than 10 ps ("truth jets") and serve as the reference for the trigger jet calibration.

The calibration of trigger jets closely followed the usual calibration procedure for offline jets [52]. The differences between trigger and offline calibrations, summarized in Fig. 3 and described in the following, arise from the differences in jet reconstruction and the information available at the trigger level. A final calibration step, the trigger/offline correction, was performed to align trigger jets to the offline jet energy scale. This allowed the treatment of trigger jets to adopt identical uncertainties to those derived during the offline jet calibration, except for flavor uncertainties, whose treatment differs from that for offline jets due to the lack of tracking information and is discussed in this section and Sec. VII. All steps up to and including the global sequential correction are applied to jets both in simulation and in data, while all subsequent steps are applied only to jets in data.

The high statistical precision of the TLA stream, with a sensitivity to signal amplitudes of the order of 10^{-4} to 10^{-3} relative to the background contribution, poses strict smoothness requirements on the jet calibration. Throughout the calibration chain, special emphasis was placed on keeping the jet response a smooth function of jet p_{T} without local features to avoid introducing peaking features into the dijet mass distribution.

Pile-up correction The first step in the calibration sequence was the jet-area-based pile-up correction, to remove additional energy from pile-up collisions. The jet area A, as a measure for the susceptibility of a given jet to additional energy from pile-up collisions, was measured for each jet by ghost-association [53,54]. The contribution of pile-up in the event was estimated from the average pile-up density $\rho = \mathrm{median}\{p_{\mathrm{T}}(j)/A(j)\}$ of the ratio of transverse momentum p_{T} and area A of all jets j in the event. The initial transverse momentum $p_{\mathrm{T}}^{\mathrm{init}}$ was corrected to

$$p_{\mathrm{T}}^{\mathrm{area}} = p_{\mathrm{T}}^{\mathrm{init}} - \rho A,$$

using the product of ρ and A as an estimate for the contribution from pile-up to the momentum of each individual jet. This correction was performed within the HLT. Therefore the trigger jets entering the TLA stream were calibrated to this scale and all subsequent calibration steps were derived and applied relative to it.

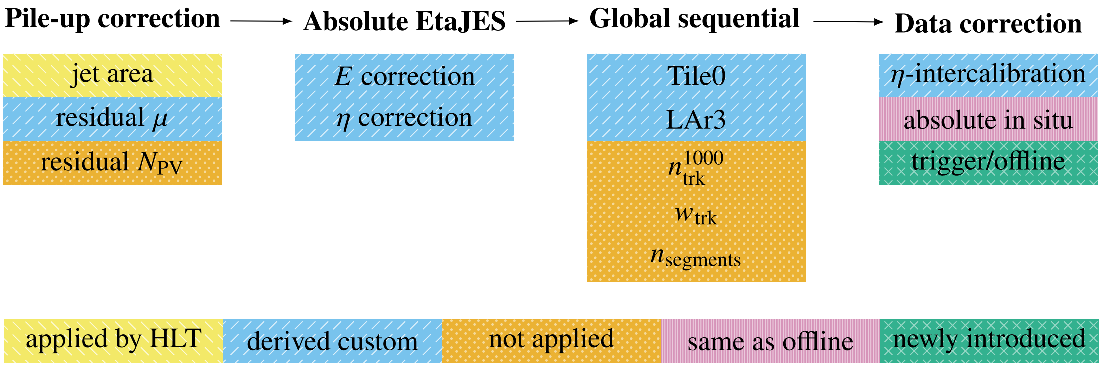

FIG. 3. Stages and substeps of the trigger jet calibration and how they differ from the offline jet calibration. Following the jet area correction performed by the HLT during data collection (yellow hatched), this analysis uses dedicated calibration steps (blue hatched) correcting for pile-up and differing energy response of hadronic signals throughout the detector. Steps of the offline calibration employing tracking are omitted due to the lack of tracking in the TLA stream (orange hatched). Trigger jets in data are further corrected with a dedicated η-intercalibration while the same absolute *in situ* calibration as derived for offline jets is applied (purple hatched). This is followed by a new trigger/offline step (green hatched) to correct for remaining differences between offline and trigger jets.

The offline jet pile-up calibration [52] procedure foresees a residual correction

$$p_{\text{T}}^{\text{res}} = p_{\text{T}}^{\text{area}} - \frac{\partial p_{\text{T}}}{\partial N_{\text{PV}}}(N_{\text{PV}} - 1) - \frac{\partial p_{\text{T}}}{\partial \mu}\mu,$$

based on the number of vertices with at least two associated tracks with $p_{\text{T}} > 500$ MeV (“primary vertices”) N_{PV} in the event and the mean number of interactions per bunch crossing μ. The former is affected only by in-time pile-up while the latter is affected by both in-time and out-of-time pile-up. Since vertex information is not recorded for the TLA stream, a calibration based on N_{PV} is not possible; hence only the μ term of the residual pile-up calibration was applied to trigger. In this and all subsequent simulation-based calibration steps, trigger and truth jets were geometrically matched by their angular distance requirement $\Delta R < 0.3$, and truth (trigger) jets were required to be isolated from all other truth (trigger) jets in the event by $\Delta R > 1.0$ ($\Delta R > 0.6$). The factor $\partial p_{\text{T}}/\partial \mu$ was determined by linear fits of $p_{\text{T}}^{\text{area}} - p_{\text{T}}^{\text{true}}$ versus μ for trigger jets with $60 < p_{\text{T}}^{\text{true}} < 80$ GeV in simulated dijet events. This was done independently for each $|\eta^{\text{truth}}| < 4.0$ interval of width 0.1.

Figure 4(a) shows that this residual step significantly decreases the dependence $\partial p_{\text{T}}/\partial \mu$ of trigger jet p_{T} with respect to μ. Figure 4(b) shows that the $\partial p_{\text{T}}/\partial N_{\text{PV}}$ dependence is unaffected by this correction. This constitutes a significant improvement on the prior ATLAS dijet TLA [12], where only the jet-area-based correction was applied.

Absolute EtaJES correction Subsequently, a simulation-based absolute calibration was applied to correct the jet energy E scale (JES) to that of truth jets. The average jet energy response after the pile-up correction

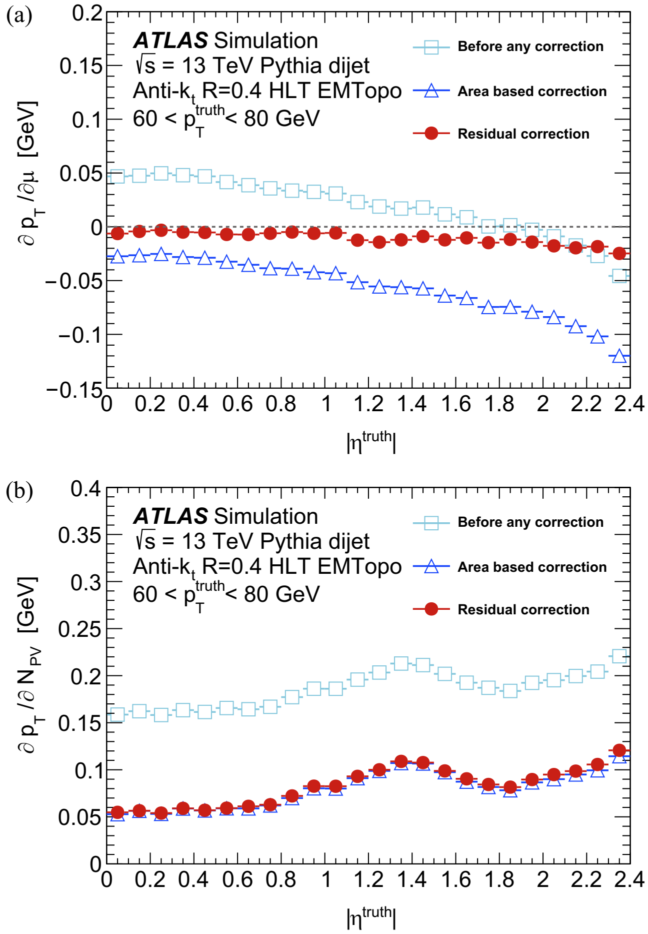

FIG. 4. Dependence of the reconstructed trigger jet p_{T} on (a) the average number of interactions per bunch crossings μ and (b) the number of primary vertices N_{PV} before (open squares) and after the two steps of pile-up calibration described in Sec. IV, the area based correction (open triangles), and residual correction (filled circles) in simulated dijet events, as a function of the pseudorapidity $|\eta^{\text{truth}}|$ of the corresponding truth jet.

was measured as $\mathcal{R}_E = \frac{E^{\text{trigger}}}{E^{\text{truth}}}$ in bins of E^{truth} and η^{det}.[2] The statistical mode of each response distribution was estimated as the mean of a fit of a Gaussian distribution to its core. Correction factors were extracted by fitting the resulting modes with the functional form

$$\mathcal{F}_{\text{JES}}(E^{\text{truth}}) = \sum_{i=0}^{N_{\max}} a_i (\ln E^{\text{truth}})^i,$$

where a_i is a free parameter. For each fit the functional order $N_{\max}$ is chosen from the interval $\{1..6\}$ such that it results in the minimal χ^2 of the fit [55]. A numerical inversion procedure was applied to obtain the factors as a function of trigger rather than truth quantities $\mathcal{F}_{\text{JES}}(E^{\text{trigger}})$, such that they can be applied to trigger jets.

Figure 5(a) shows that the value of the response before applying the EtaJES correction is highly dependent on the pseudorapidity η^{det} and can change by up to 50%. This is partly due to varying instrumentation across different detector regions, which can result in a bias in the direction of reconstructed jets, especially the pseudorapidity η, towards better-instrumented regions of the detector. Hence, an additional correction to the pseudorapidity was applied to compensate for this effect. It was derived in the same way as the energy correction, but using the difference $\Delta\eta = \eta^{\text{trigger}} - \eta^{\text{truth}}$ rather than the response $\mathcal{R}_E$.

Closure is defined as the difference between the response to unity after the correction is applied. Figure 5(a) shows that the EtaJES achieves a closure of 5% in the forward region (and significantly below that in the central region) for jets with $E > 80$ GeV.

Global sequential correction Up to this point both energy and direction of reconstructed trigger jets are calibrated on average. A global sequential correction (GSC) was then applied to improve the response of individual populations of jets, e.g. jets that differ in the fraction of energy deposited in different calorimeter components, while leaving the overall response unchanged. As a result, the overall resolution improves, as measured by the width of Gaussian distributions fit to the cores of the response. ATLAS typically applies a GSC [52] based on five variables:

(i) f_{Tile0}: The fraction of jet energy measured in the first layer of the hadronic tile calorimeter;
(ii) f_{LAr3}: The fraction of jet energy measured in the third layer of the electromagnetic Liquid Argon calorimeter;
(iii) n_{trk}^{1000}: The number of $p_{\text{T}} > 1$ GeV tracks associated with the jet;

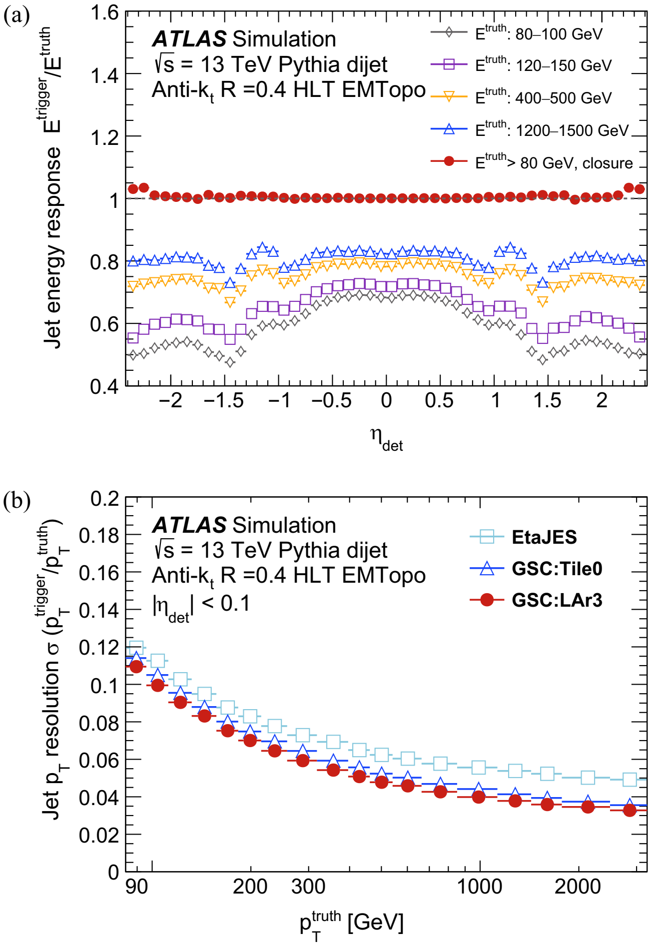

FIG. 5. (a) Trigger jet energy response, $E^{\text{trigger}}/E^{\text{truth}}$, in bins of detector pseudorapidity η^{det} of the truth jet p_{T}, $p_{\text{T}}^{\text{truth}}$, before applying the EtaJES calibration step (open markers in ranges of truth jet energy from 80 to 1500 GeV) and closure after applying the correction (filled circles). (b) Resolution $\sigma(p_{\text{T}}^{\text{trigger}}/p_{\text{T}}^{\text{truth}})$ of trigger jet transverse momentum p_{T} as a function of truth jet p_{T} after the EtaJES calibration step (open squares) and after each of the calorimeter-based GSC steps, Tile0 (open triangles) and LAr3 (filled circles) in the central detector η bin $|\eta^{\text{det}}| < 0.1$.

(iv) w_{trk}: The p_{T}-weighted transverse distance of tracks to the jet axis;
(v) n_{segments}: The p_{T}-weighted transverse distance of muon spectrometer segments to the jet axis.

Due to their dependence on tracking information, the last three of these variables were not available to the TLA stream. Consequently, only the first two steps of the normal sequence, involving the variables f_{Tile0} and f_{LAr3}, were performed for the trigger jet calibration. One GSC variable after the other, the response $\mathcal{R}_{p_{\text{T}}}$ distribution of trigger jets with respect to matched truth jets was constructed in bins of $p_{\text{T}}^{\text{truth}}$, η^{det}, and the GSC variable and extracted as the mean of a fit to a Gaussian distribution. For each η bin, a 2-dimensional (2-D) Gaussian kernel smoothing in $p_{\text{T}}^{\text{truth}}$ and the GSC variable was performed on the resulting

---

[2] η^{det} is the jet pseudorapidity pointing from the geometric centre of the detector. Its use reduces ambiguity as to which region of the detector is measuring the jet.

average response. The final calibration factors as a function of trigger jet p_T and η were determined by numerical inversion. This procedure was performed for each GSC variable sequentially, i.e., the response of the second variable was constructed after applying the correction based on the first variable. Figure 5(b) illustrates both steps of the GSC improve the trigger jet resolution.

The subsequent tracking-based steps of the offline GSC sequence are intended to correct for the differences between quark- and gluon-initiated jets. These latter steps use variables (n_trk^{1000}, w_trk, n_segments) available only from offline reconstruction. They typically produce corrections that are smaller than the prior steps in the offline sequence. Despite lacking the track-based steps, the trigger GSC described here achieves similar resolution to the offline GSC, with 10% at 100 GeV and 4% at 2 TeV [56]. Flavor uncertainties for trigger jets were rederived to account for the absence of the tracking-based steps and found to be a factor of two larger than for offline jets, as discussed in Sec. VII.

Data correction In addition to the three Monte-Carlo derived calibration steps described so far, a data-based calibration was applied, with the goal of correcting for residual differences in the energy scale in data that are not modeled in the simulation. While the Monte-Carlo derived calibrations rely on simulated particle-level jets as reference, the data corrections rely on reconstructed objects with well-calibrated response as reference to calibrate objects with less well-understood response, taking advantage of the overall transverse momentum balance in an event. For offline jets, this correction comprises two parts: the η-intercalibration and the absolute *in situ* calibration. The former balances jets in the forward detector regions with those in the better instrumented central region while the latter balances jets in hadronic recoil events with a photon or leptonically decaying Z boson. For trigger jets, an additional step, the trigger/offline correction, was derived.

The η-intercalibration is designed to accommodate for the effect that the response of central jets is usually better constrained than that of forward jets. The ratio of data / simulation response is constructed in bins of η and p_T and a 2-D smoothing is applied. A jet-vertex-tagger (JVT) [57] requirement of >0.59 is applied based on the JVT score of $\Delta R < 0.3$ matched offline jets. To better constrain the smoothness, for trigger jets a 7-parameter poly-log functional form fit

$$\mathcal{F}_\mathrm{intercal}(p_\mathrm{T}) = \sum_{i=-3}^{3} a_i \log^i(p_\mathrm{T})$$

was used instead of the 2-D Gaussian kernel used for the offline jet *in situ* calibration. Apart from this, the procedure of deriving the η-intercalibration here does not differ from that for offline jets. The resulting distribution is applied as a calibration curve for jets with $|\eta| > 0.8$.

For offline jets, an absolute *in situ* calibration was obtained from the p_T balance of events with jets recoiling against well-measured objects in data. Forward jets were corrected based on them recoiling against central jets in dijet events while central jets were corrected based on recoils with photons in $\gamma +$ jets events or leptons in $Z(\rightarrow \text{leptons}) +$ jets events. The previous calibration steps bring the trigger jets to nearly identical scales as offline jets, which allowed the trigger jet calibration to use the same *in situ* calibration factors as offline jets.

An additional calibration step correcting trigger jets to the scale of offline jets was applied to account for any residual differences between the two calibrations. This calibration was derived independently for each year (2016, 2017, 2018) and the two TLA data samples (J50, J100) accounting for the different pile-up conditions of each year of data taking, and the fact that the J50 L1 trigger was mostly active at the end of LHC fills (again with differing pile-up conditions). To store both trigger and offline jets for an event, the HLT must have accepted the event, initiating the offline jet reconstruction. Different single-jet HLT triggers were used depending on the $p_\mathrm{T}^\mathrm{avg} = (p_\mathrm{T}^\mathrm{lead} + p_\mathrm{T}^\mathrm{sublead})/2$, the average transverse momentum of p_T-leading and subleading offline jets $\Delta R < 0.2$ matched to trigger jets, ensuring the triggers are fully efficient. Event-by-event prescale factors were taken into account to correct the population of jets for bias from triggers whose varying prescale factors led to differing distributions of instantaneous luminosity.

A response $\mathcal{R} = p_\mathrm{T}^\mathrm{trigger}/p_\mathrm{T}^\mathrm{offline}$ was derived as the mean of fits in data to a Gaussian distribution in bins of $p_\mathrm{T}^\mathrm{avg}$. The motivation for deriving and validating the trigger/offline calibration in bins of $p_\mathrm{T}^\mathrm{avg}$ rather than single-jet p_T was to account for the varying flavor composition of the two leading jets per event such that the correction factor is valid for the whole dijet system. A numerical inversion, followed by a 2-D Gaussian kernel smoothing, was performed to determine the final calibration factor in bins of trigger jet $p_\mathrm{T}^\mathrm{avg}$ and η.

A trigger/offline p_T closure of the order of 1% is observed inclusively in η. After the correction, it improves to be within 0.5% over the full $p_\mathrm{T}^\mathrm{avg}$ range. The closure in individual η regions before (after) the correction is within 2% (1%). The final statistical interpretation of the analysis is performed on the invariant mass of the dijet system m_{jj}. Hence, the m_{jj} response of trigger relative to offline jets, Fig. 6, was measured as a final calibration check. Similarly to the p_T closure, the m_{jj} closure improves from 1% to 0.5% after applying the correction. The differences in closure between J50 and J100 arise from the difference in pile-up conditions, with the J50 selection activated exclusively during lower instantaneous luminosity. The remaining non-closure is approximately constant in m_{jj} and small in comparison to the dominant jet energy scale uncertainties discussed in Sec. VII.

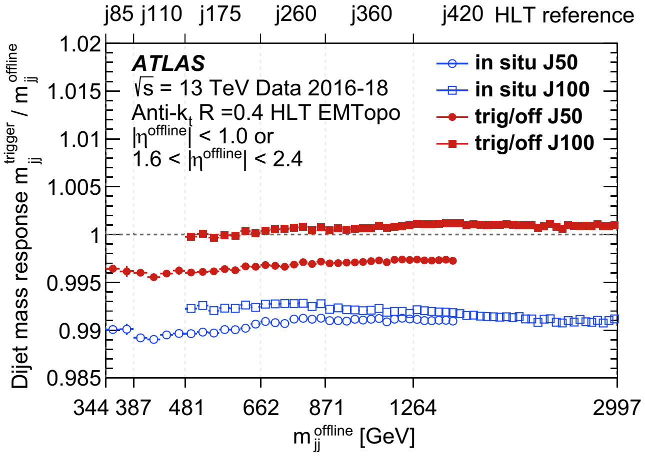

FIG. 6. Improvement in the ratio of trigger to offline dijet mass, $m_{jj}^{\mathrm{trigger}}/m_{jj}^{\mathrm{offline}}$, for the J50 (circles) and J100 (squares) samples before (open markers after the *in situ* calibration step) and after applying the trigger/offline calibration (filled markers) for all years of data taking combined. For offline jets, different leading jet $p_{\mathrm{T}} > X$ GeV thresholds (abbreviated as jX) are required which are fully efficient for a given $m_{jj}^{\mathrm{offline}}$ region. Each region is exclusively populated by one trigger based on the offline jet p_{T}. Events where either leading or subleading jet fall into the region $1.0 < |\eta^{\mathrm{offline}}| < 1.6$ are excluded to avoid jets whose calibration performance is not sufficient, as discussed in Sec. V.

V. EVENT SELECTION

For the search and the data-driven background estimate, events from the TLA stream were selected that contain at least two trigger jets, each with $p_{\mathrm{T}} > 85$ GeV and $|\eta| < 2.4$. The two highest p_{T} jets satisfy $|y^*| < 0.6$. This requirement suppresses the background from SM multijet processes, which grows with y^* due to t-channel poles at leading order. This value was chosen to optimise the Poisson signal significance $(S/\sqrt{B})$ in simulated data for the Z' signals of mass 350 to 1000 GeV.

After these selections, events with either jet having $1.0 < |\eta| < 1.6$ were discarded. These jets overlap with a narrow "tile gap" region between hadronic calorimeters that is instrumented only by a thin set of gap and cryostat scintillators [58]. In this region, the jet calibration procedure described in the previous section is unable to reach the performance demanded by the statistical uncertainties in the TLA sample.

Events meeting these requirements were further divided into "J100" and "J50" signal regions by the L1 trigger that collected them. For J50-triggered data, events with calibrated m_{jj} below 344 GeV were discarded to remove data sculpted by the kinematic requirements of the L1 trigger. For J100-triggered data, the minimum allowed m_{jj} was 481 GeV. These thresholds were chosen from dedicated measurements of the trigger efficiencies as a function of data-taking period, jet p_{T} and dijet m_{jj}, varying the y^* requirement from 0.3 to no requirement at all, to ensure that these triggers reached full efficiency throughout the mass regions used for the search.

Figure 7 shows the m_{jj} distributions for the two signal regions after these selections, in variable-width bins which correspond to the calibrated trigger jet m_{jj} resolution in simulation.

VI. BACKGROUND ESTIMATE

The SM background in the search is dominated by nonpeaking multijet processes convolved with a smooth detector response. The estimate of this background began with an ansatz

$$f(x) = p_1(1-x)^{p_2} x^{\sum_{i=3}^{N} p_i \log^{(i-3)}(x)} \left(1 + \sum_{j=1}^{n_{\mathrm{syst}}} \theta_j \sum_{k=1}^{5} c_{jk} x^k\right), \tag{1}$$

where $x \equiv m_{jj}/\sqrt{s}$ and N is a fixed number of shape parameters. Dijet mass distributions were found to be well described by expressions similar to Eq. (1) ($\theta_j = 0$) in prior dijet searches with lower statistical precision [13,59–64]. In Eq. (1), systematic uncertainties in the background shape due to the jet calibration are modeled via nuisance parameters θ_j and modulating factors c_{jk} derived from simulation as described in Sec. VII. The m_{jj} data in Fig. 7 in each signal region were divided into 1 GeV fixed-size bins and fit with Eq. (1) using a RooFit+RooStats-based [65,66] framework to obtain the parameters p_i and nuisance parameters θ_j.

Fits to this ansatz were validated separately for each of the two signal regions. As constructing a sample of multijet processes with equivalent statistical uncertainties to Fig. 7 was computationally impractical with the ATLAS detector simulation, the fit procedure for fixed N was validated on pseudodata. This pseudodata was generated by applying Poisson fluctuations matching the statistical uncertainties in Fig. 7 to fits of both subsamples and the entirety of the data in Fig. 7 with Eq. (1) with $N_0 = N + 1$ parameters. A χ^2 probability larger than 1% was required for the N_0 fit to ensure that the pseudodata accurately models the shape of the m_{jj} distribution in data. In case of a localised excess prohibiting the χ^2 threshold being reached, the excess region would have been masked from the N_0 fit to ensure that pseudodata corresponding to a background-only m_{jj} distribution could be generated.

Fits to the pseudodata confirm the χ^2 goodness-of-fit follows the eponymous distribution, which was used to assign the quoted χ^2 probabilities with the number of degrees of freedom given by the difference between the number of bins and the number of unconstrained parameters in the fit.

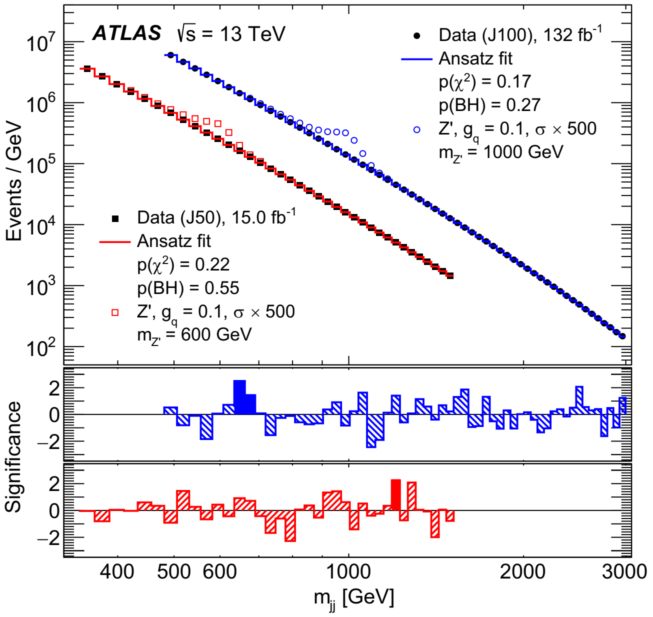

FIG. 7. Observed m_{jj} distributions for the J50 (filled squares) and J100 (filled circles) signal regions, using the variable-width bins and analysis selections described in the text. In the upper panel, the histograms indicate the background estimates from each ansatz fit, integrated over each bin. Predictions for two Z' signals are shown above the fit (open markers), normalized to 500 times the predicted cross section for a quark coupling $g_q = 0.1$ for visibility. The lower panels show the significance of the differences between data and background estimates in units of the statistical uncertainties in the numbers of events in each bin. The regions identified as the most significant by BumpHunter are indicated in the bottom panel as contiguous solid-filled bins. The p-value for the fit χ^2 and global value from BumpHunter are indicated in the legends for each of the two signal regions.

The fit for fixed N was validated by performing signal-plus-background fits with freely floating signal amplitude on the generated N_0 pseudodata, using a set of the signal masses and shapes tested in Sec. VIII. As the pseudodata is generated to behave like the background-only distribution, the expectation of the signal amplitude extracted in these fits is zero. Any deviation from this indicates a bias in the fit and is thus labeled spurious signal. For each signal hypothesis it was validated on the ensemble of fits to pseudodata that the spurious signal is Gaussian-distributed with a mean of the order of the standard deviation. Additionally, N_0 pseudodata with signals injected were used to verify that the background component of the fit is not significantly affected by the presence of signal and that the extracted signal amplitude corresponds to the injected amplitude within uncertainties. Notably, the machine precision of the bin-wise evaluation of the negative log-likelihood in RooFit was found insufficient for the unprecedented numbers of events shown in Fig. 7; the Gaussian limits of the Poissonian terms in the likelihood were used to avoid this limitation.

From the previously validated fit strategies, an F-test [67] was performed to determine the value of N for which further increasing the fit flexibility does not significantly improve the χ^2 goodness-of-fit. This test was performed on the data in both signal regions independently with a threshold of $p(F) > 0.05$. It resulted in a choice of $N = 6$ in both signal regions.

VII. UNCERTAINTIES

Systematic uncertainties in the jet energy scale and resolution were considered for both the signal and the background contributions. They were evaluated on the simulated Z' and dijet samples mentioned in Sec. III, respectively, by independently varying 40 nuisance parameters up and down within their uncertainties on a jet-by-jet basis. The jet energy scale uncertainties with the highest impact on the signal template Z' fits are shown in Fig. 8. All uncertainties except for the flavor composition, flavor response, and η-intercalibration modelling uncertainty are identical to those derived for offline jets.

The flavor uncertainties were rederived as in Ref. [56],

$$\sigma^{\text{flavor}}_{\text{response}} = f_g \sigma_{R_g},$$

$$\sigma^{\text{flavor}}_{\text{composition}} = \frac{\sigma_{f_g} |R_q - R_g|}{f_g R_g + (1 - f_g) R_q},$$

where R_q and R_g are the fraction of light quarks and gluons that were estimated from Pythia 8 dijet simulated events. The gluon response modeling uncertainty σ_{R_g} was obtained as the maximum difference between the gluon response in Pythia 8, HERWIG [68,69], and Sherpa [70,71] simulated events. The gluon fraction f_g was set to a constant value of 50% with a conservative estimate on its uncertainty of $\sigma_{f_g} = 100\% f_g$. The flavor uncertainties are the dominant jet uncertainties and mainly arise due to the lack of tracking information which, for the offline jet calibration, is key to aligning the response of quark- and gluon-initiated jets [56].

To parameterise the impact of the uncertainties on the signal, a double-sided Crystal Ball function [72,73] was fit to the nominal and systematically varied Z' m_{jj} distributions. The impact of each nuisance parameter on the mean and the width of the Gaussian core of the function is assigned as systematic uncertainty both for Z' and Gaussian-shaped resonance signals. The dominant sources of uncertainty in the mean of the signal is the uncertainty in the jet flavor composition ranging from 8 to 20 GeV with rising signal mass. It is followed by the jet flavor response and the *in situ* uncertainties both ranging approximately from 2 to 12 GeV. The uncertainty in the width of the signal is small with all nuisance parameters having a sub-GeV impact.

For the systematic uncertainties in the background, the ratios of the systematic up and down variations of the m_{jj}

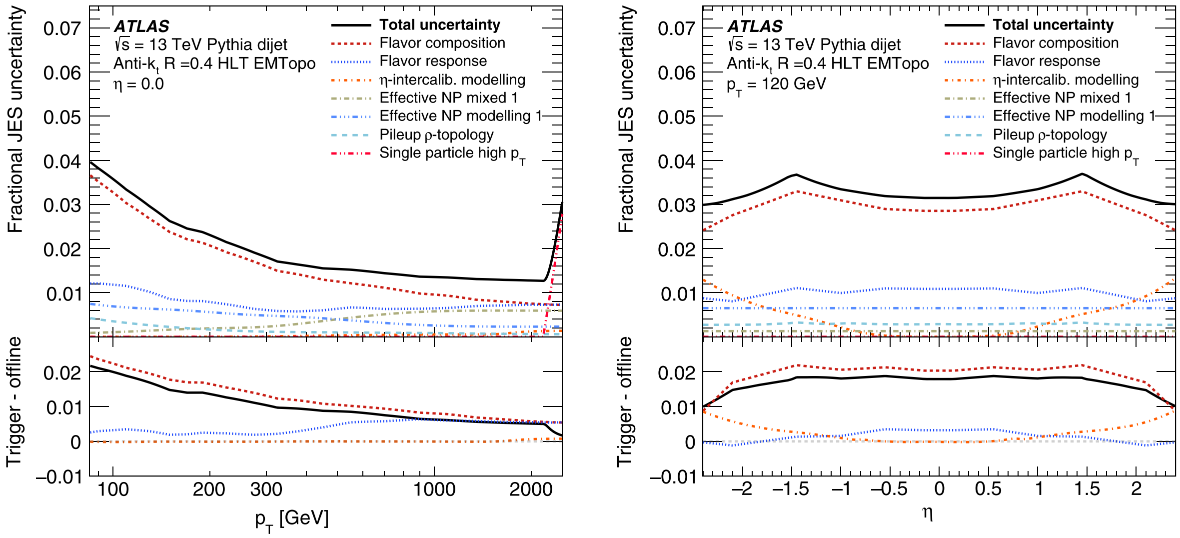

FIG. 8. Total systematic uncertainty in the energy scale of trigger jets (solid lines) and the most significant of 40 components considered, as a function of jet (a) p_T and (b) η. The bottom panel shows the absolute differences between trigger jet and offline jet uncertainties for the total uncertainty and the three components that were rederived for trigger jets. Uncertainties in the flavor composition of jets (uppermost dashed line) are the largest contribution to the total uncertainty and the source of the largest difference with the offline calibration uncertainty, arising due to the absence of tracking information used in the offline GSC to correct for different responses to quark- and gluon-initiated jets.

distributions to the nominal distribution were symmetrized and fit with a fifth degree polynomial. The resulting coefficients c_{jk}, $k = 1\ldots5$ for each systematic uncertainty j were used to parameterise the shape of this uncertainty in the background ansatz in Eq. (1), treating it as fully correlated across m_{jj}. The amplitude for each is a nuisance parameter θ_j with normal constraint in the likelihood.

The systematic uncertainties in the signal and background contributions were treated as uncorrelated.

The amount of spurious signal determined for each signal hypothesis and mass was considered as an additional systematic uncertainty by adding a separate signal component of identical shape and a Gaussian-constrained amplitude to the signal-plus-background fits. This uncertainty was found to be up to the order of half the statistical uncertainty in the signal amplitude for most Z' and narrow Gaussian-shaped resonance signals and up to 170% of the statistical uncertainty for wide resonances. The extreme cases are largely driven by the inclusion of the systematic uncertainties in background shape in the ansatz fit, which increases the fit flexibility and the spurious signal. The resulting impact on the sensitive signal cross section ranges from being negligible to up to an 80% increase, depending on signal shape and mass.

The uncertainties originating from the total collected luminosity of the samples were below 1% and have a negligible effect on the presented results [74]. No other normalisation uncertainties in the Z' cross section for a given coupling constant g_q is applied for comparability with other results probing Z' dijet resonances.

VIII. RESULTS AND EXCLUSION LIMITS

The m_{jj} distributions obtained from the J50 and J100 signal regions are shown in Fig. 7, overlaid with the corresponding background estimates from the $N = 6$ ansatz fits including background systematic variations. The residuals for each fit are shown in the lower panels. The observed distributions are well described by the fits. The fits yield a χ^2 p-value of 0.22 in the J50 signal region and 0.17 in the J100 region.

The BumpHunter algorithm [75,76] was used to further assess localised excesses in either m_{jj} distribution. The algorithm scans all possible contiguous mass intervals across the binned distribution, from a width of one bin to a width of half of the distribution. For each interval, it computes the probability of a Poisson fluctuation of the fitted background estimate at least as large as that observed. The algorithm identifies the bins spanning 1186 to 1225 GeV for the J50 distribution and 635 to 690 GeV for the J100 distribution, indicated by solid-filled bins in the residual panels of the figure, as the most significant discrepancies in each signal region. The global p-values, determined from a large number of pseudoexperiments drawn from the background estimate, are 0.55 for the J50 signal region and 0.27 for the J100 signal region. Thus, this yields no evidence of a localised contribution to the mass distributions in excess of the background.

The data were used to constrain the Z' model discussed in Sec. III and the cross section times acceptance times branching ratio to two jets, $\sigma \times A \times \mathrm{BR}$, of a hypothetical signal that produces a Gaussian-shaped contribution to the observed m_{jj} distribution.

Samples of Z' events were simulated for $m_{Z'}$ values of 200, 350, 450, 650, 1000, and 2000 GeV and at coupling values $g_q = 0.2$ and lower. Before parton shower effects, the intrinsic width of this Z' is 1.6%–1.9% depending on $m_{Z'}$ for $g_q = 0.2$ and at the lower coupling values reached by the search ranges from 0.1% of its mass for a mass of 850 GeV and $g_q = 0.04$ to 0.6% for a mass of 1.8 TeV and $g_q = 0.11$. The decrease in width with decreasing coupling was negligible compared to the detector m_{jj} resolution and therefore neglected. The selection acceptance in the J50 signal region for a signal with $g_q = 0.1$ is 12% for a mass of 375 GeV and in the J100 signal region is 17% for a mass of 600 GeV and 32% for a mass of 2.0 TeV. Each simulated sample was analysed identically to data to obtain an m_{jj} line-shape. Line-shapes for additional values of $m_{Z'}$ were generated by linear interpolation of the parameters of a double-sided Crystal Ball function fit to these distributions.

Limits were also calculated for hypothetical signals with a Gaussian-shaped m_{jj} distribution at mean mass m_G and three different widths from 5% to 15% of the mean mass.

To derive the constraints on these two types of signals from the m_{jj} distribution, a frequentist method [77] was applied to the data and simulation of signals at a series of discrete masses to set 95% $\mathrm{CL_S}$ [78] upper limits on the cross section times acceptance times branching ratio to jets for the signals.

Only the signal region with the stronger expected limit was used for each signal mass. The J100 sample, with higher statistical power, constrained masses above 600 GeV, while lower masses, more affected by fit uncertainties due to the minimum m_{jj} requirement, were constrained using the J50 sample.

When evaluating the likelihood to derive limits, the parameters of the background fit function were left floating to take its flexibility given different signal hypotheses into account. This constitutes a more rigorous consideration of background uncertainties than commonly employed in previous searches, including Ref. [12]. In comparison to the previous approach, this results in more conservative exclusion limits that are better comparable to other recent dijet searches with similar background fits [14,16,22]. Pseudodata injected with signals of various amplitudes were used to validate proper coverage of the derived limits with all systematic uncertainties considered.

Figure 9 shows the constraints on the two types of signals. The observed exclusion limits are in good agreement with the background-only expectation. The largest localised excess is observed for a Z' signal with a mass of $m_{Z'} = 650$ GeV, corresponding to a 3.4σ local significance. This translates to a global significance of 2.2σ as determined using the expected number of "downcrossings" in pseudodata [79]. Fluctuations in the expected limits arise from the mass-dependent spurious signal systematic uncertainty. The model-dependent constraints in Fig. 9(b) are also overlaid with results from the ATLAS Run 2 dijet resonance search using offline jets [13], in the overlapping

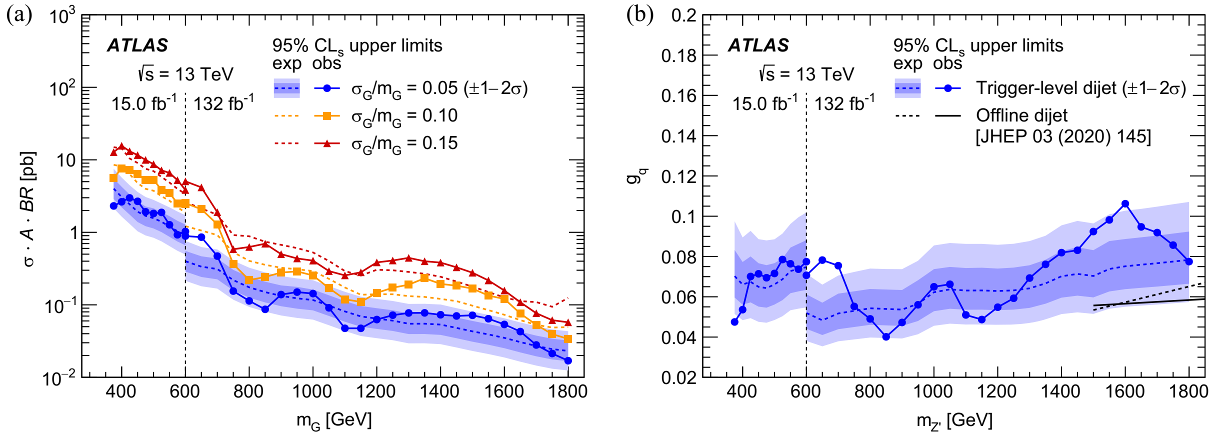

FIG. 9. Observed 95% $\mathrm{CL_S}$ upper limits on (a) the production cross section times acceptance times branching ratio to jets, $\sigma \cdot A \cdot \mathrm{BR}$, of Gaussian-shaped signals of 5% (filled circles), 10% (squares) and 15% (triangles) width relative to their peak mass, m_G, and (b) the value of the coupling to quarks, g_q, of the Z' model as a function of the resonance mass $m_{Z'}$ (filled circles). Also shown are the corresponding expected upper limits predicted for the case the m_{jj} distribution is observed to be identical to the background prediction in each bin (dashed lines). For the narrowest Gaussian-shaped (5%) and Z' signals, the shaded bands indicate the 1σ (darker band) and 2σ (lighter band) envelopes of outcomes expected for Poisson fluctuations around the background expectation. The uncertainty bands for wider Gaussian-shaped signals are of similar relative size. Overlaid on panel (b) are the observed (darker solid line) and expected (darker dashed line) upper limits from the ATLAS Run-2 search using the main stream and offline jets [13], which benefits from tracking information and data in the tile gap region of the calorimeter. Limits are derived independently from the J50 and J100 samples for m_{jj} below and above 600 GeV, respectively, denoted by the vertical dashed line, as discussed in the text.

Z' mass range above 1500 GeV. The limits from the offline search are stronger as it uses tracking information in the jet calibration and has an increased acceptance from including jets in the entire $|\eta| < 2.4$ range.

The limits on Gaussian-shaped resonances are intended to be used to constrain signal models other than the Z' when PDF and nonperturbative effects can be safely truncated or neglected and, after applying the resonance selection, the reconstructed m_{jj} distribution predicted by the model approaches a Gaussian distribution. For example, for sufficiently narrow resonances, the intrinsic line-shape can be neglected because the experimental m_{jj} resolution and parton shower tail determines the observed line-shape of the signal. Signals with an intrinsic width much smaller than 5% should be compared to the limit for width equal to 5% of its mass, corresponding to 1–2 times the experimental resolution over the m_{jj} range considered. Signals with larger widths should be compared with the limit that corresponds most closely to the width of the peak predicted by the model. More instructions can be found in Appendix A of Ref. [63].

IX. CONCLUSION

This paper describes a search for sub-TeV dijet resonances in 132 fb^{-1} of proton–proton collisions with a center-of-mass energy of $\sqrt{s} = 13$ TeV recorded by the ATLAS detector at the Large Hadron Collider. The search was performed using the TLA technique on trigger jets to obtain up to 75 times greater numbers of events than available to conventional searches for dijet resonances in the targeted mass range. This search exploits an end-of-fill triggering scheme and the L1Topo topological trigger processor to extend the search region further into the electroweak mass region, from 600 GeV to 375 GeV. This result also improves the statistical treatment of the data-derived background estimate used by the previous result [12], allowing the high-statistics background from each sample to be modeled with a single functional fit.

The dijet invariant mass distribution recorded with the TLA technique exhibits no significant local excesses above a data-derived estimate of the smoothly falling distribution predicted by the Standard Model. The data were used to derive 95% confidence-level upper limits on the couplings of a leptophobic Z' model with axial-vector couplings to quarks, which range from $g_q < 0.04$ to $g_q < 0.11$ depending on $m_{Z'}$, and on the cross section for new processes that would produce a Gaussian-shaped contribution to the dijet mass distribution. The latter constraints exclude Gaussian-shaped contributions if the effective cross section times acceptance times branching ratio exceeds values ranging from approximately 17 fb to 16 pb depending on resonance mass and width. These results extend and improve the limits obtained from partial Run 2 data to lower production cross sections and coupling values, superseding the previous ATLAS result [12]. They constitute the strongest published exclusion limits on dijet resonances in the mass range 375 to 425 GeV and 700 to 1500 GeV [13,15,22].

ACKNOWLEDGMENTS

We thank CERN for the very successful operation of the LHC and its injectors, as well as the support staff at CERN and at our institutions worldwide without whom ATLAS could not be operated efficiently. The crucial computing support from all WLCG partners is acknowledged gratefully, in particular from CERN, the ATLAS Tier-1 facilities at TRIUMF/SFU (Canada), NDGF (Denmark, Norway, Sweden), CC-IN2P3 (France), KIT/GridKA (Germany), INFN-CNAF (Italy), NL-T1 (Netherlands), PIC (Spain), RAL (UK) and BNL (USA), the Tier-2 facilities worldwide and large non-WLCG resource providers. Major contributors of computing resources are listed in Ref. [80]. We gratefully acknowledge the support of ANPCyT, Argentina; YerPhI, Armenia; ARC, Australia; BMWFW and FWF, Austria; ANAS, Azerbaijan; CNPq and FAPESP, Brazil; NSERC, NRC and CFI, Canada; CERN; ANID, Chile; CAS, MOST and NSFC, China; Minciencias, Colombia; MEYS CR, Czech Republic; DNRF and DNSRC, Denmark; IN2P3-CNRS and CEA-DRF/IRFU, France; SRNSFG, Georgia; BMFTR, HGF and MPG, Germany; GSRI, Greece; RGC and Hong Kong SAR, China; ICHEP and Academy of Sciences and Humanities, Israel; INFN, Italy; MEXT and JSPS, Japan; CNRST, Morocco; NWO, Netherlands; RCN, Norway; MNiSW, Poland; FCT, Portugal; MNE/IFA, Romania; MSTDI, Serbia; MSSR, Slovakia; ARIS and MVZI, Slovenia; DSI/NRF, South Africa; MICIU/AEI, Spain; SRC and Wallenberg Foundation, Sweden; SERI, SNSF and Cantons of Bern and Geneva, Switzerland; NSTC, Taipei; TENMAK, Türkiye; STFC/UKRI, United Kingdom; DOE and NSF, United States of America. Individual groups and members have received support from BCKDF, CANARIE, CRC and DRAC, Canada; CERN-CZ, FORTE and PRIMUS, Czech Republic; COST, ERC, ERDF, Horizon 2020, ICSC-NextGenerationEU and Marie Skłodowska-Curie Actions, European Union; Investissements d'Avenir Labex, Investissements d'Avenir Idex and ANR, France; DFG and AvH Foundation, Germany; Herakleitos, Thales and Aristeia programmes cofinanced by EU-ESF and the Greek NSRF, Greece; BSF-NSF and MINERVA, Israel; NCN and NAWA, Poland; La Caixa Banking Foundation, CERCA Programme Generalitat de Catalunya and PROMETEO and GenT Programmes Generalitat Valenciana, Spain; Göran Gustafssons Stiftelse, Sweden; The Royal Society and Leverhulme Trust, United Kingdom. In addition, individual members wish to acknowledge support from CERN: European Organization for Nuclear Research (CERN DOCT); Chile: Agencia Nacional de Investigación y Desarrollo

(FONDECYT 1230812, FONDECYT 1240864, Fondecyt 3240661); China: Chinese Ministry of Science and Technology (MOST-2023YFA1605700, MOST-2023YFA1609300), National Natural Science Foundation of China (NSFC-12175119, NSFC 12275265); Czech Republic: Czech Science Foundation (GACR-24-11373S), Ministry of Education Youth and Sports (ERC-CZ-LL2327, FORTE CZ.02.01.01/00/22_008/0004632), PRIMUS Research Programme (PRIMUS/21/SCI/017); EU: H2020 European Research Council (ERC-101002463); European Union: European Research Council (BARD No. 101116429, ERC-948254, ERC 101089007), European Regional Development Fund (SMASH COFUND 101081355, SLO ERDF), European Union, Future Artificial Intelligence Research (FAIR-NextGenerationEU PE00000013), Italian Center for High Performance Computing, Big Data and Quantum Computing (ICSC, NextGenerationEU); France: Agence Nationale de la Recherche (ANR-21-CE31-0022, ANR-22-EDIR-0002, ANR-24-CE31-0504-01); Germany: Deutsche Forschungsgemeinschaft (DFG-469666862, DFG-CR 312/5-2); China: Research Grants Council (GRF); Italy: Istituto Nazionale di Fisica Nucleare (ICSC, NextGenerationEU), Ministero dell'Università e della Ricerca (NextGenEU 153D23001490006 M4C2.1.1, NextGenEU I53D23000820006 M4C2.1.1, NextGenEU I53D23001490006 M4C2.1.1, SOE2024_0000023); Japan: Japan Society for the Promotion of Science (JSPS KAKENHI JP22H01227, JSPS KAKENHI JP22H04944, JSPS KAKENHI JP22KK0227, JSPS KAKENHI JP24K23939, JSPS KAKENHI JP24KK0251, JSPS KAKENHI JP25H00650, JSPS KAKENHI JP25H01291, JSPS KAKENHI JP25K01023); Norway: Research Council of Norway (RCN-314472); Poland: Ministry of Science and Higher Education (IDUB AGH, POB8, D4 no 9722), Polish National Science Centre (NCN 2021/42/E/ST2/00350, NCN OPUS 2023/51/B/ST2/02507, NCN UMO-2019/34/E/ST2/00393, UMO-2022/47/O/ST2/00148, UMO-2023/49/B/ST2/04085, UMO-2023/51/B/ST2/00920, UMO-2024/53/N/ST2/00869); Portugal: Foundation for Science and Technology (FCT); Spain: Ministry of Science and Innovation (MCIN & NextGenEU PCI2022-135018-2, MICIN & FEDER PID2021-125273NB, RYC2019-028510-I, RYC2020-030254-I, RYC2021-031273-I, RYC2022-038164-I); Sweden: Carl Trygger Foundation (Carl Trygger Foundation CTS 22:2312), Swedish Research Council (Swedish Research Council 2023-04654, VR 2021-03651, VR 2022-03845, VR 2022-04683, VR 2023-03403, VR 2024-05451), Knut and Alice Wallenberg Foundation (KAW 2018.0458, KAW 2022.0358, KAW 2023.0366); Switzerland: Swiss National Science Foundation (SNSF-PCEFP2_194658); United Kingdom: Royal Society (NIF-R1-231091); United States of America: U.S. Department of Energy (ECA DE-AC02-76SF00515), Neubauer Family Foundation.

DATA AVAILABILITY

The public release of data supporting the findings of this article will follow the CERN Open Data Policy [81]. The values of relevant plots and tables associated with this article are stored in HEPData [82].

---

[1] G. Arnison *et al.*, Experimental observation of isolated large transverse energy electrons with associated missing energy at $\sqrt{s} = 540$ GeV, Phys. Lett. **122B**, 103 (1983).

[2] M. Banner *et al.*, Observation of single isolated electrons of high transverse momentum in events with missing transverse energy at the CERN $\bar{p}p$ collider, Phys. Lett. **122B**, 476 (1983).

[3] G. Arnison *et al.*, Experimental observation of lepton pairs of invariant mass around 95 GeV/c^2 at the CERN SPS collider, Phys. Lett. **126B**, 398 (1983).

[4] UA2 Collaboration, Evidence for $Z^0 \to e^+e^-$ at the CERN $\bar{p}p$ collider, Phys. Lett. **129B**, 130 (1983).

[5] CDF Collaboration, Observation of top quark production in $\bar{p}p$ collisions, Phys. Rev. Lett. **74**, 2626 (1995).

[6] D0 Collaboration, Observation of the top quark, Phys. Rev. Lett. **74**, 2632 (1995).

[7] ATLAS Collaboration, Observation of a new particle in the search for the standard model Higgs boson with the ATLAS detector at the LHC, Phys. Lett. B **716**, 1 (2012).

[8] CMS Collaboration, Observation of a new boson at a mass of 125 GeV with the CMS experiment at the LHC, Phys. Lett. B **716**, 30 (2012).

[9] ATLAS Collaboration, The ATLAS experiment at the CERN large hadron collider, J. Instrum. **3**, S08003 (2008).

[10] L. Evans and P. Bryant, LHC machine, J. Instrum. **3**, S08001 (2008).

[11] CMS Collaboration, The CMS experiment at the CERN LHC, J. Instrum. **3**, S08004 (2008).

[12] ATLAS Collaboration, Search for low-mass dijet resonances using trigger-level jets with the ATLAS detector in pp collisions at $\sqrt{s} = 13$ TeV, Phys. Rev. Lett. **121**, 081801 (2018).

[13] ATLAS Collaboration, Search for new resonances in mass distributions of jet pairs using 139 fb^{-1} of pp collisions at $\sqrt{s} = 13$ TeV with the ATLAS detector, J. High Energy Phys. 03 (2020) 145.

[14] CMS Collaboration, Search for narrow and broad dijet resonances in proton–proton collisions at $\sqrt{s} = 13$ TeV and constraints on dark matter mediators and other new particles, J. High Energy Phys. 08 (2018) 130.

[15] CMS Collaboration, Search for narrow resonances in dijet final states at $\sqrt{s} = 8$ TeV with the novel CMS technique of data scouting, Phys. Rev. Lett. **117**, 031802 (2016).

[16] CMS Collaboration, Search for dijet resonances using events with three jets in proton–proton collisions at $\sqrt{s} = 13$ TeV, Phys. Lett. B **805**, 135448 (2020).

[17] LHCb Collaboration, The LHCb detector at the LHC, J. Instrum. **3**, S08005 (2008).

[18] R. Aaij *et al.*, Tesla: An application for real-time data analysis in high energy physics, Comput. Phys. Commun. **208**, 35 (2016).

[19] R. Aaij *et al.*, A comprehensive real-time analysis model at the LHCb experiment, J. Instrum. **14**, P04006 (2019).

[20] ATLAS Collaboration, Search for light resonances decaying to boosted quark pairs and produced in association with a photon or a jet in proton–proton collisions at $\sqrt{s} = 13$ TeV with the ATLAS detector, Phys. Lett. B **788**, 316 (2019).

[21] ATLAS Collaboration, Search for boosted low-mass resonances decaying into hadrons produced in association with a photon in pp collisions at $\sqrt{s} = 13$ TeV with the ATLAS detector, J. High Energy Phys. 01 (2025) 099.

[22] ATLAS Collaboration, Search for low-mass resonances decaying into two jets and produced in association with a photon or a jet at $\sqrt{s} = 13$ TeV with the ATLAS detector, Phys. Rev. D **110**, 032002 (2024).

[23] ATLAS Collaboration, Search for low-mass resonances decaying into two jets and produced in association with a photon using pp collisions at $\sqrt{s} = 13$ TeV with the ATLAS detector, Phys. Lett. B **795**, 56 (2019).

[24] ATLAS Collaboration, Search for dijet resonances in events with an isolated charged lepton using $\sqrt{s} = 13$ TeV proton–proton collision data collected by the ATLAS detector, J. High Energy Phys. 06 (2020) 151.

[25] ATLAS Collaboration, Search for resonances in the mass distribution of jet pairs with one or two jets identified as b-jets in proton–proton collisions at $\sqrt{s} = 13$ TeV with the ATLAS detector, Phys. Rev. D **98**, 032016 (2018).

[26] CMS Collaboration, Search for narrow resonances in the b-tagged dijet mass spectrum in proton–proton collisions at $\sqrt{s} = 13$ TeV, Phys. Rev. D **108**, 012009 (2023).

[27] CMS Collaboration, Search for low-mass quark–antiquark resonances produced in association with a photon at $\sqrt{s} = 13$ TeV, Phys. Rev. Lett. **123**, 231803 (2019).

[28] ATLAS Collaboration, ATLAS insertable B-layer: Technical design report, Reports No. ATLAS-TDR-19, No. CERN-LHCC-2010-013, 2010, https://cds.cern.ch/record/1291633; Addendum: Reports No. ATLAS-TDR-19-ADD-1, No. CERN-LHCC-2012-009, 2012, https://cds.cern.ch/record/1451888.

[29] B. Abbott *et al.*, Production and integration of the ATLAS Insertable B-Layer, J. Instrum. **13**, T05008 (2018).

[30] ATLAS Collaboration, Performance of the ATLAS trigger system in 2015, Eur. Phys. J. C **77**, 317 (2017).

[31] ATLAS Collaboration, Performance of the ATLAS level-1 topological trigger in Run 2, Eur. Phys. J. C **82**, 7 (2022).

[32] ATLAS Collaboration, Operation of the ATLAS trigger system in Run 2, J. Instrum. **15**, P10004 (2020).

[33] ATLAS Collaboration, The performance of the jet trigger for the ATLAS detector during 2011 data taking, Eur. Phys. J. C **76**, 526 (2016).

[34] ATLAS Collaboration, Selection of jets produced in 13 TeV proton–proton collisions with the ATLAS detector, Report No. ATLAS-CONF-2015-029, 2015, https://cds.cern.ch/record/2037702.

[35] ATLAS Collaboration, Software and computing for Run 3 of the ATLAS experiment at the LHC, Eur. Phys. J. C **85**, 234 (2025).

[36] ATLAS Collaboration, ATLAS data quality operations and performance for 2015–2018 data-taking, J. Instrum. **15**, P04003 (2020).

[37] ATLAS Collaboration, Monitoring and data quality assessment of the ATLAS liquid argon calorimeter, J. Instrum. **9**, P07024 (2014).

[38] T. Sjöstrand *et al.*, An introduction to Pythia 8.2, Comput. Phys. Commun. **191**, 159 (2015).

[39] ATLAS Collaboration, ATLAS Pythia 8 tunes to 7 TeV data, Report No. ATL-PHYS-PUB-2014-021, 2014, https://cds.cern.ch/record/1966419.

[40] R. D. Ball *et al.* (NNPDF Collaboration), Parton distributions with LHC data, Nucl. Phys. **B867**, 244 (2013).

[41] T. Sjöstrand, S. Mrenna, and P. Skands, A brief introduction to Pythia 8.1, Comput. Phys. Commun. **178**, 852 (2008).

[42] ATLAS Collaboration, The Pythia 8 A3 tune description of ATLAS minimum bias and inelastic measurements incorporating the Donnachie–Landshoff diffractive model, Report No. ATL-PHYS-PUB-2016-017, 2016, https://cds.cern.ch/record/2206965.

[43] S. Agostinelli *et al.*, Geant4—a simulation toolkit, Nucl. Instrum. Methods Phys. Res., Sect. A **506**, 250 (2003).

[44] ATLAS Collaboration, The ATLAS simulation infrastructure, Eur. Phys. J. C **70**, 823 (2010).

[45] D. Abercrombie *et al.*, Dark matter benchmark models for early LHC Run-2 searches: Report of the ATLAS/CMS dark matter forum, Phys. Dark Universe **27**, 100371 (2020).

[46] J. Alwall *et al.*, The automated computation of tree-level and next-to-leading order differential cross sections, and their matching to parton shower simulations, J. High Energy Phys. 07 (2014) 079.

[47] D. J. Lange, The EvtGen particle decay simulation package, Nucl. Instrum. Methods Phys. Res., Sect. A **462**, 152 (2001).

[48] M. Chala, F. Kahlhoefer, M. McCullough, G. Nardini, and K. Schmidt-Hoberg, Constraining dark sectors with monojets and dijets, J. High Energy Phys. 07 (2015) 089.

[49] ATLAS Collaboration, Topological cell clustering in the ATLAS calorimeters and its performance in LHC Run 1, Eur. Phys. J. C **77**, 490 (2017).

[50] M. Cacciari, G. P. Salam, and G. Soyez, The anti-k_t jet clustering algorithm, J. High Energy Phys. 04 (2008) 063.

[51] M. Cacciari, G. P. Salam, and G. Soyez, FastJet user manual, Eur. Phys. J. C **72**, 1896 (2012).

[52] ATLAS Collaboration, Jet energy scale measurements and their systematic uncertainties in proton–proton collisions at $\sqrt{s} = 13$ TeV with the ATLAS detector, Phys. Rev. D **96**, 072002 (2017).

[53] M. Cacciari, G. P. Salam, and G. Soyez, The catchment area of jets, J. High Energy Phys. 04 (2008) 005.

[54] M. Cacciari and G. P. Salam, Pileup subtraction using jet areas, Phys. Lett. B **659**, 119 (2008).

[55] ATLAS Collaboration, Jet energy measurement with the ATLAS detector in proton–proton collisions at $\sqrt{s} = 7$ TeV, Eur. Phys. J. C **73**, 2304 (2013).

[56] ATLAS Collaboration, Jet energy scale and resolution measured in proton–proton collisions at $\sqrt{s} = 13$ TeV with the ATLAS detector, Eur. Phys. J. C **81**, 689 (2021).

[57] ATLAS Collaboration, Performance of pile-up mitigation techniques for jets in pp collisions at $\sqrt{s} = 8$ TeV using the ATLAS detector, Eur. Phys. J. C **76**, 581 (2016).

[58] ATLAS Collaboration, Operation and performance of the ATLAS tile calorimeter in LHC Run 2, Eur. Phys. J. C **84**, 1313 (2024).

[59] CDF Collaboration, Search for new particles decaying into dijets in proton-antiproton collisions at $\sqrt{s} = 1.96$ TeV, Phys. Rev. D **79**, 112002 (2009).

[60] ATLAS Collaboration, Search for new particles in two-jet final states in 7 TeV proton–proton collisions with the ATLAS detector at the LHC, Phys. Rev. Lett. **105**, 161801 (2010).

[61] CMS Collaboration, Search for resonances in the dijet mass spectrum from 7 TeV pp collisions at CMS, Phys. Lett. B **704**, 123 (2011).

[62] ATLAS Collaboration, A search for new physics in dijet mass and angular distributions in pp collisions at $\sqrt{s} = 7$ TeV measured with the ATLAS detector, New J. Phys. **13**, 053044 (2011).

[63] ATLAS Collaboration, Search for new phenomena in the dijet mass distribution using pp collision data at $\sqrt{s} = 8$ TeV with the ATLAS detector, Phys. Rev. D **91**, 052007 (2015).

[64] CMS Collaboration, Search for high mass dijet resonances with a new background prediction method in proton–proton collisions at $\sqrt{s} = 13$ TeV, J. High Energy Phys. 05 (2020) 033.

[65] W. Verkerke and D. Kirkby, The RooFit toolkit for data modeling, arXiv:physics/0306116.

[66] L. Moneta *et al.*, The RooStats Project, arXiv:1009.1003.

[67] ATLAS Collaboration, Recommendations for the modeling of smooth backgrounds, Report No. ATL-PHYS-PUB-2020-028, 2020, https://cds.cern.ch/record/2743717.

[68] M. Bähr *et al.*, Herwig++ physics and manual, Eur. Phys. J. C **58**, 639 (2008).

[69] J. Bellm *et al.*, Herwig 7.0/Herwig++ 3.0 release note, Eur. Phys. J. C **76**, 196 (2016).

[70] S. Höche, F. Krauss, S. Schumann, and F. Siegert, QCD matrix elements and truncated showers, J. High Energy Phys. 05 (2009) 053.

[71] E. Bothmann *et al.*, Event generation with Sherpa 2.2, SciPost Phys. **7**, 034 (2019).

[72] M. Oreglia, A study of the reactions $\psi' \to \gamma\gamma\psi$, Report No. SLAC-R-0236, 1980, https://www.slac.stanford.edu/pubs/slacreports/reports13/slac-r-236.pdf.

[73] ATLAS Collaboration, Search for scalar diphoton resonances in the mass range 65–600 GeV with the ATLAS detector in pp collision data at $\sqrt{s} = 8$ TeV, Phys. Rev. Lett. **113**, 171801 (2014).

[74] ATLAS Collaboration, Luminosity determination in pp collisions at $\sqrt{s} = 13$ TeV using the ATLAS detector at the LHC, Eur. Phys. J. C **83**, 982 (2023).

[75] CDF Collaboration, Global search for new physics with 2.0 fb^{-1} at CDF, Phys. Rev. D **79**, 011101 (2009).

[76] G. Choudalakis, On hypothesis testing, trials factor, hypertests and the BumpHunter, arXiv:1101.0390.

[77] G. Cowan, K. Cranmer, E. Gross, and O. Vitells, Asymptotic formulae for likelihood-based tests of new physics, Eur. Phys. J. C **71**, 1554 (2011).

[78] A. L. Read, Presentation of search results: The CL_s technique, J. Phys. G **28**, 2693 (2002).

[79] E. Gross and O. Vitells, Trial factors for the look elsewhere effect in high energy physics, Eur. Phys. J. C **70**, 525 (2010).

[80] ATLAS Collaboration, ATLAS computing acknowledgements, Report No. ATL-SOFT-PUB-2025-001, 2025, https://cds.cern.ch/record/2922210.

[81] CERN, CERN Open Data Policy for the LHC Experiments, CERN-OPEN-2020-013, 2020, https://cds.cern.ch/record/2745133.

[82] ATLAS Collaboration, Search for electroweak-scale dijet resonances using trigger-level analysis with the ATLAS detector in 132 fb^{-1} of pp collisions at $\sqrt{s} = 13$ TeV (Version 1), 2025, 10.17182/hepdata.161624.v1.

G. Aad,[104] E. Aakvaag,[17] B. Abbott,[123] S. Abdelhameed,[119a] K. Abeling,[55] N. J. Abicht,[49] S. H. Abidi,[30]
M. Aboelela,[45] A. Aboulhorma,[36e] H. Abramowicz,[157] Y. Abulaiti,[120] B. S. Acharya,[69a,69b,b] A. Ackermann,[63a]
C. Adam Bourdarios,[4] L. Adamczyk,[87a] S. V. Addepalli,[149] M. J. Addison,[103] J. Adelman,[118] A. Adiguzel,[22c]
T. Adye,[137] A. A. Affolder,[139] Y. Afik,[40] M. N. Agaras,[13] A. Aggarwal,[102] C. Agheorghiesei,[28c] F. Ahmadov,[39,c]
S. Ahuja,[97] S. Ahuja,[169] X. Ai,[143b] G. Aielli,[76a,76b] A. Aikot,[169] M. Ait Tamlihat,[36e] B. Aitbenchikh,[36a]
M. Akbiyik,[102] T. P. A. Åkesson,[100] A. V. Akimov,[151] D. Akiyama,[174] N. N. Akolkar,[25] S. Aktas,[172]
G. L. Alberghi,[24b] J. Albert,[171] U. Alberti,[20] P. Albicocco,[53] G. L. Albouy,[60] S. Alderweireldt,[52]
Z. L. Alegria,[124] M. Aleksa,[37] I. N. Aleksandrov,[39] C. Alexa,[28b] T. Alexopoulos,[10] F. Alfonsi,[24b] M. Algren,[56]
M. Alhroob,[173] B. Ali,[135] H. M. J. Ali,[93,d] S. Ali,[32] S. W. Alibocus,[94] M. Aliev,[34c] G. Alimonti,[71a]
W. Alkakhi,[55] C. Allaire,[66] B. M. M. Allbrooke,[152] D. R. Allen,[124] J. S. Allen,[103] J. F. Allen,[52] P. P. Allport,[21]
A. Aloisio,[72a,72b] F. Alonso,[92] C. Alpigiani,[142] Z. M. K. Alsolami,[93] A. Alvarez Fernandez,[102]

M. Alves Cardoso,[56] M. G. Alviggi,[72a,72b] M. Aly,[103] Y. Amaral Coutinho,[83b] A. Ambler,[106] C. Amelung,[37]
M. Amerl,[103] C. G. Ames,[111] T. Amezza,[130] D. Amidei,[108] B. Amini,[54] K. Amirie,[161] A. Amirkhanov,[39]
S. P. Amor Dos Santos,[133a] K. R. Amos,[169] D. Amperiadou,[158] S. An,[84] C. Anastopoulos,[145] T. Andeen,[11]
J. K. Anders,[94] A. C. Anderson,[59] A. Andreazza,[71a,71b] S. Angelidakis,[9] A. Angerami,[42] A. V. Anisenkov,[39]
A. Annovi,[74a] C. Antel,[37] E. Antipov,[151] M. Antonelli,[53] F. Anulli,[75a] M. Aoki,[84] T. Aoki,[159] M. A. Aparo,[152]
L. Aperio Bella,[48] M. Apicella,[31] C. Appelt,[157] A. Apyan,[27] M. Arampatzi,[10] S. J. Arbiol Val,[88] C. Arcangeletti,[53]
A. T. H. Arce,[51] J-F. Arguin,[110] S. Argyropoulos,[158] J.-H. Arling,[48] O. Arnaez,[4] H. Arnold,[151] G. Artoni,[75a,75b]
H. Asada,[113] K. Asai,[121] S. Asatryan,[179] N. A. Asbah,[37] R. A. Ashby Pickering,[173] A. M. Aslam,[97]
K. Assamagan,[30] R. Astalos,[29a] K. S. V. Astrand,[100] S. Atashi,[165] R. J. Atkin,[34a] H. Atmani,[36f]
P. A. Atmasiddha,[131] K. Augsten,[135] A. D. Auriol,[41] V. A. Austrup,[103] A. S. Avad,[96] G. Avolio,[37] K. Axiotis,[56]
A. Azzam,[13] D. Babal,[29b] H. Bachacou,[138] K. Bachas,[158,e] A. Bachiu,[35] E. Bachmann,[50] M. J. Backes,[63a]
A. Badea,[40] T. M. Baer,[108] P. Bagnaia,[75a,75b] M. Bahmani,[19] D. Bahner,[54] K. Bai,[126] J. T. Baines,[137]
L. Baines,[96] O. K. Baker,[178] E. Bakos,[16] D. Bakshi Gupta,[8] L. E. Balabram Filho,[83b] V. Balakrishnan,[123]
R. Balasubramanian,[4] E. M. Baldin,[38] P. Balek,[87a] E. Ballabene,[24b,24a] F. Balli,[138] L. M. Baltes,[63a]
W. K. Balunas,[33] J. Balz,[102] I. Bamwidhi,[119b] E. Banas,[88] M. Bandieramonte,[132] A. Bandyopadhyay,[25]
S. Bansal,[25] L. Barak,[157] M. Barakat,[48] E. L. Barberio,[107] D. Barberis,[18b] M. Barbero,[104] M. Z. Barel,[117]
T. Barillari,[112] M-S. Barisits,[37] T. Barklow,[149] P. Baron,[136] D. A. Baron Moreno,[103] A. Baroncelli,[62]
A. J. Barr,[129] J. D. Barr,[98] F. Barreiro,[101] J. Barreiro Guimarães da Costa,[14] M. G. Barros Teixeira,[133a] S. Barsov,[38]
F. Bartels,[63a] R. Bartoldus,[149] A. E. Barton,[93] P. Bartos,[29a] M. Baselga,[49] S. Bashiri,[88] A. Bassalat,[66,f]
M. J. Basso,[162a] S. Bataju,[45] R. Bate,[170] R. L. Bates,[59] S. Batlamous,[101] M. Battaglia,[139] D. Battulga,[19]
M. Bauce,[75a,75b] M. Bauer,[79] P. Bauer,[25] L. T. Bayer,[48] L. T. Bazzano Hurrell,[31] J. B. Beacham,[112] T. Beau,[130]
J. Y. Beaucamp,[92] P. H. Beauchemin,[164] P. Bechtle,[25] H. P. Beck,[20,g] K. Becker,[173] A. J. Beddall,[82]
V. A. Bednyakov,[39] C. P. Bee,[151] L. J. Beemster,[16] M. Begalli,[83d] M. Begel,[30] J. K. Behr,[48] J. F. Beirer,[37]
F. Beisiegel,[25] M. Belfkir,[119b] G. Bella,[157] L. Bellagamba,[24b] A. Bellerive,[35] C. D. Bellgraph,[68] P. Bellos,[21]
K. Beloborodov,[38] I. Benaoumeur,[21] D. Benchekroun,[36a] F. Bendebba,[36a] Y. Benhammou,[157]
K. C. Benkendorfer,[61] L. Beresford,[48] M. Beretta,[53] E. Bergeaas Kuutmann,[167] N. Berger,[4] B. Bergmann,[135]
J. Beringer,[18a] G. Bernardi,[5] C. Bernius,[149] F. U. Bernlochner,[25] A. Berrocal Guardia,[13] T. Berry,[97] P. Berta,[136]
A. Berthold,[50] A. Berti,[133a] R. Bertrand,[104] S. Bethke,[112] A. Betti,[75a,75b] A. J. Bevan,[96] L. Bezio,[56]
N. K. Bhalla,[54] S. Bharthuar,[112] S. Bhatta,[151] P. Bhattarai,[149] Z. M. Bhatti,[120] K. D. Bhide,[54] V. S. Bhopatkar,[124]
R. M. Bianchi,[132] G. Bianco,[24b,24a] O. Biebel,[111] M. Biglietti,[77a] C. S. Billingsley,[45] Y. Bimgdi,[36f] M. Bindi,[55]
A. Bingham,[177] A. Bingul,[22b] C. Bini,[75a,75b] G. A. Bird,[33] M. Birman,[175] M. Biros,[136] S. Biryukov,[152]
T. Bisanz,[49] E. Bisceglie,[24b,24a] J. P. Biswal,[137] D. Biswas,[147] I. Bloch,[48] A. Blue,[59] U. Blumenschein,[96]
V. S. Bobrovnikov,[39] L. Boccardo,[57b,57a] M. Boehler,[54] B. Boehm,[172] D. Bogavac,[13] A. G. Bogdanchikov,[38]
L. S. Boggia,[130] V. Boisvert,[97] P. Bokan,[37] T. Bold,[87a] M. Bomben,[5] M. Bona,[96] M. Boonekamp,[138]
A. G. Borbély,[59] I. S. Bordulev,[38] G. Borissov,[93] D. Bortoletto,[129] D. Boscherini,[24b] M. Bosman,[13]
K. Bouaouda,[36a] N. Bouchhar,[169] L. Boudet,[4] J. Boudreau,[132] E. V. Bouhova-Thacker,[93] D. Boumediene,[41]
R. Bouquet,[57b,57a] A. Boveia,[122] J. Boyd,[37] D. Boye,[30] I. R. Boyko,[39] L. Bozianu,[56] J. Bracinik,[21] N. Brahimi,[4]
G. Brandt,[177] O. Brandt,[33] B. Brau,[105] J. E. Brau,[126] R. Brener,[175] L. Brenner,[117] R. Brenner,[167] S. Bressler,[175]
G. Brianti,[78a,78b] D. Britton,[59] D. Britzger,[112] I. Brock,[25] R. Brock,[109] G. Brooijmans,[42] A. J. Brooks,[68]
E. M. Brooks,[162b] E. Brost,[30] L. M. Brown,[171,162a] L. E. Bruce,[61] T. L. Bruckler,[129]
P. A. Bruckman de Renstrom,[88] B. Brüers,[48] A. Bruni,[24b] G. Bruni,[24b] D. Brunner,[47a,47b] M. Bruschi,[24b]
N. Bruscino,[75a,75b] T. Buanes,[17] Q. Buat,[142] D. Buchin,[112] A. G. Buckley,[59] O. Bulekov,[82] B. A. Bullard,[149]
S. Burdin,[94] C. D. Burgard,[49] A. M. Burger,[91] B. Burghgrave,[8] O. Burlayenko,[54] J. Burleson,[168]
J. C. Burzynski,[148] E. L. Busch,[42] V. Büscher,[102] P. J. Bussey,[59] O. But,[25] J. M. Butler,[26] C. M. Buttar,[59]
J. M. Butterworth,[98] W. Buttinger,[137] C. J. Buxo Vazquez,[109] A. R. Buzykaev,[39] S. Cabrera Urbán,[169]
L. Cadamuro,[66] H. Cai,[37] Y. Cai,[24b,114c,24a] Y. Cai,[114a] V. M. M. Cairo,[37] O. Cakir,[3a] N. Calace,[37]
P. Calafiura,[18a] G. Calderini,[130] P. Calfayan,[35] L. Calic,[100] G. Callea,[59] L. P. Caloba,[83b] D. Calvet,[41] S. Calvet,[41]
R. Camacho Toro,[130] S. Camarda,[37] D. Camarero Munoz,[27] P. Camarri,[76a,76b] C. Camincher,[171] M. Campanelli,[98]
A. Camplani,[43] V. Canale,[72a,72b] A. C. Canbay,[3a] E. Canonero,[97] J. Cantero,[169] Y. Cao,[168] F. Capocasa,[27]

M. Capua,[44b,44a] A. Carbone,[71a,71b] R. Cardarelli,[76a] J. C. J. Cardenas,[8] M. P. Cardiff,[27] G. Carducci,[44b,44a]
T. Carli,[37] G. Carlino,[72a] J. I. Carlotto,[13] B. T. Carlson,[132,h] E. M. Carlson,[171] J. Carmignani,[94]
L. Carminati,[71a,71b] A. Carnelli,[4] M. Carnesale,[37] S. Caron,[116] E. Carquin,[140g] I. B. Carr,[107] S. Carrá,[73a,73b]
G. Carratta,[24b,24a] C. Carrion Martinez,[169] A. M. Carroll,[126] M. P. Casado,[13,i] P. Casolaro,[72a,72b] M. Caspar,[48]
W. R. Castiglioni,[40] F. L. Castillo,[4] L. Castillo Garcia,[13] V. Castillo Gimenez,[169] N. F. Castro,[133a,133e]
A. Catinaccio,[37] J. R. Catmore,[128] T. Cavaliere,[4] V. Cavaliere,[30] L. J. Caviedes Betancourt,[23b] E. Celebi,[82]
S. Cella,[37] V. Cepaitis,[56] K. Cerny,[125] A. S. Cerqueira,[83a] A. Cerri,[74a,74b,j] L. Cerrito,[76a,76b] F. Cerutti,[18a]
B. Cervato,[71a,71b] A. Cervelli,[24b] G. Cesarini,[53] S. A. Cetin,[82] P. M. Chabrillat,[130] R. Chakkappai,[66]
S. Chakraborty,[173] A. Chambers,[61] J. Chan,[18a] W. Y. Chan,[159] J. D. Chapman,[33] E. Chapon,[138]
B. Chargeishvili,[155b] D. G. Charlton,[21] C. Chauhan,[136] Y. Che,[114a] S. Chekanov,[6] G. A. Chelkov,[39,k] B. Chen,[157]
B. Chen,[171] H. Chen,[114a] H. Chen,[30] J. Chen,[144a] J. Chen,[148] M. Chen,[129] S. Chen,[89] S. J. Chen,[114a]
X. Chen,[144a] X. Chen,[15,l] Z. Chen,[62] C. L. Cheng,[176] H. C. Cheng,[64a] S. Cheong,[149] A. Cheplakov,[39]
E. Cherepanova,[117] R. Cherkaoui El Moursli,[36e] E. Cheu,[7] K. Cheung,[65] L. Chevalier,[138] V. Chiarella,[53]
G. Chiarelli,[74a] G. Chiodini,[70a] A. S. Chisholm,[21] A. Chitan,[28b] M. Chitishvili,[169] M. V. Chizhov,[39,m] K. Choi,[11]
Y. Chou,[142] E. Y. S. Chow,[116] K. L. Chu,[175] M. C. Chu,[64a] X. Chu,[14,114c] Z. Chubinidze,[53] J. Chudoba,[134]
J. J. Chwastowski,[88] D. Cieri,[112] K. M. Ciesla,[87a] V. Cindro,[95] A. Ciocio,[18a] F. Cirotto,[72a,72b] Z. H. Citron,[175]
M. Citterio,[71a] D. A. Ciubotaru,[28b] A. Clark,[56] P. J. Clark,[52] N. Clarke Hall,[98] C. Clarry,[161] S. E. Clawson,[48]
C. Clement,[47a,47b] L. Clissa,[24b,24a] Y. Coadou,[104] M. Cobal,[69a,69c] A. Coccaro,[57b] R. F. Coelho Barrue,[133a]
R. Coelho Lopes De Sa,[105] S. Coelli,[71a] L. S. Colangeli,[161] B. Cole,[42] P. Collado Soto,[101] J. Collot,[60]
R. Coluccia,[70a,70b] P. Conde Muiño,[133a,133g] M. P. Connell,[34c] S. H. Connell,[34c] E. I. Conroy,[129]
M. Contreras Cossio,[11] F. Conventi,[72a,n] A. M. Cooper-Sarkar,[129] L. Corazzina,[75a,75b] F. A. Corchia,[24b,24a]
A. Cordeiro Oudot Choi,[142] L. D. Corpe,[41] M. Corradi,[75a,75b] F. Corriveau,[106,o] A. Cortes-Gonzalez,[159]
M. J. Costa,[169] F. Costanza,[4] D. Costanzo,[145] J. Couthures,[4] G. Cowan,[97] K. Cranmer,[176] L. Cremer,[49]
D. Cremonini,[24b,24a] S. Crépé-Renaudin,[60] F. Crescioli,[130] T. Cresta,[73a,73b] M. Cristinziani,[147]
M. Cristoforetti,[78a,78b] E. Critelli,[98] V. Croft,[117] G. Crosetti,[44b,44a] A. Cueto,[101] H. Cui,[98] Z. Cui,[7]
B. M. Cunnett,[152] W. R. Cunningham,[59] F. Curcio,[169] J. R. Curran,[52] M. J. Da Cunha Sargedas De Sousa,[57b,57a]
J. V. Da Fonseca Pinto,[83b] C. Da Via,[103] W. Dabrowski,[87a] T. Dado,[37] S. Dahbi,[154] T. Dai,[108] D. Dal Santo,[20]
C. Dallapiccola,[105] M. Dam,[43] G. D'amen,[30] V. D'Amico,[111] J. R. Dandoy,[35] M. D'Andrea,[57b,57a]
D. Dannheim,[37] G. D'anniballe,[74a,74b] M. Danninger,[148] V. Dao,[151] G. Darbo,[57b] S. J. Das,[30] F. Dattola,[48]
S. D'Auria,[71a,71b] A. D'Avanzo,[72a,72b] T. Davidek,[136] J. Davidson,[173] I. Dawson,[96] K. De,[8]
C. De Almeida Rossi,[161] R. De Asmundis,[72a] N. De Biase,[48] S. De Castro,[24b,24a] N. De Groot,[116] P. de Jong,[117]
H. De la Torre,[118] A. De Maria,[114a] A. De Salvo,[75a] U. De Sanctis,[76a,76b] F. De Santis,[70a,70b] A. De Santo,[152]
J. B. De Vivie De Regie,[60] J. Debevc,[95] D. V. Dedovich,[39] J. Degens,[94] A. M. Deiana,[45] J. Del Peso,[101]
L. Delagrange,[130] F. Deliot,[138] C. M. Delitzsch,[49] M. Della Pietra,[72a,72b] D. Della Volpe,[56] A. Dell'Acqua,[37]
L. Dell'Asta,[71a,71b] M. Delmastro,[4] C. C. Delogu,[57b,57a] P. A. Delsart,[60] S. Demers,[178] M. Demichev,[39]
S. P. Denisov,[38] H. Denizli,[22a,p] M. G. Depala,[94] L. D'Eramo,[41] D. Derendarz,[88] F. Derue,[130] P. Dervan,[94,a]
A. M. Desai,[1] K. Desch,[25] F. A. Di Bello,[74a,74b] A. Di Ciaccio,[76a,76b] L. Di Ciaccio,[4] A. Di Domenico,[75a,75b]
C. Di Donato,[72a,72b] A. Di Girolamo,[37] G. Di Gregorio,[66] A. Di Luca,[78a,78b] B. Di Micco,[77a,77b] R. Di Nardo,[77a,77b]
K. F. Di Petrillo,[40] M. Diamantopoulou,[35] F. A. Dias,[117] M. A. Diaz,[140a,140b] A. R. Didenko,[39] M. Didenko,[169]
S. D. Diefenbacher,[18a] E. B. Diehl,[108] S. Díez Cornell,[48] C. Diez Pardos,[147] C. Dimitriadi,[150] A. Dimitrievska,[21]
A. Dimri,[151] Y. Ding,[62] J. Dingfelder,[25] T. Dingley,[129] I-M. Dinu,[28b] S. J. Dittmeier,[63b] F. Dittus,[37]
M. Divisek,[136] B. Dixit,[94] F. Djama,[104] T. Djobava,[155b] C. Doglioni,[103,100] A. Dohnalova,[29a] Z. Dolezal,[136]
K. Domijan,[87a] K. M. Dona,[40] M. Donadelli,[83d] B. Dong,[109] J. Donini,[41] A. D'Onofrio,[72a,72b] M. D'Onofrio,[94]
J. Dopke,[137] A. Doria,[72a] N. Dos Santos Fernandes,[133a] I. A. Dos Santos Luz,[83e] P. Dougan,[103] M. T. Dova,[92]
A. T. Doyle,[59] M. P. Drescher,[55] E. Dreyer,[175] I. Drivas-koulouris,[10] M. Drnevich,[120] D. Du,[62] T. A. du Pree,[117]
Z. Duan,[114a] M. Dubau,[4] F. Dubinin,[39] M. Dubovsky,[29a] E. Duchovni,[175] G. Duckeck,[111] P. K. Duckett,[98]
O. A. Ducu,[28b] D. Duda,[52] A. Dudarev,[37] M. M. Dudek,[88] E. R. Duden,[27] M. D'uffizi,[103] L. Duflot,[66]
M. Dührssen,[37] I. Duminica,[28g] A. E. Dumitriu,[28b] M. Dunford,[63a] K. Dunne,[47a,47b] A. Duperrin,[104]
H. Duran Yildiz,[3a] A. Durglishvili,[155b] G. I. Dyckes,[18a] M. Dyndal,[87a] B. S. Dziedzic,[37] Z. O. Earnshaw,[152]

G. H. Eberwein,[129] B. Eckerova,[29a] S. Eggebrecht,[55] E. Egidio Purcino De Souza,[83e] G. Eigen,[17] K. Einsweiler,[18a]
T. Ekelof,[167] P. A. Ekman,[100] S. El Farkh,[36b] Y. El Ghazali,[62] H. El Jarrari,[106] A. El Moussaouy,[36a] D. Elitez,[37]
M. Ellert,[167] F. Ellinghaus,[177] T. A. Elliot,[97] N. Ellis,[37] J. Elmsheuser,[30] M. Elsawy,[119a] M. Elsing,[37]
D. Emeliyanov,[137] Y. Enari,[84] S. Epari,[110] D. Ernani Martins Neto,[88] F. Ernst,[37] M. Escalier,[66] C. Escobar,[169]
E. Etzion,[157] G. Evans,[133a,133b] H. Evans,[68] L. S. Evans,[48] A. Ezhilov,[38] S. Ezzarqtouni,[36a] F. Fabbri,[24b,24a]
L. Fabbri,[24b,24a] G. Facini,[98] V. Fadeyev,[139] R. M. Fakhrutdinov,[38] D. Fakoudis,[102] S. Falciano,[75a]
L. F. Falda Ulhoa Coelho,[27] F. Fallavollita,[112] G. Falsetti,[44b,44a] J. Faltova,[136] C. Fan,[168] K. Y. Fan,[64b] Y. Fan,[14]
Y. Fang,[14,114c] M. Fanti,[71a,71b] M. Faraj,[69a,69b] Z. Farazpay,[99] A. Farbin,[8] A. Farilla,[77a] K. Farman,[154]
T. Farooque,[109] J. N. Farr,[178] M. S. Farrington,[61] S. M. Farrington,[137,52] F. Fassi,[36e] D. Fassouliotis,[9] L. Fayard,[66]
P. Federic,[136] P. Federicova,[134] O. L. Fedin,[38,k] M. Feickert,[176] L. Feligioni,[104] D. E. Fellers,[18a] C. Feng,[143a]
Y. Feng,[14] Z. Feng,[117] M. J. Fenton,[165] L. Ferencz,[48] B. Fernandez Barbadillo,[93] P. Fernandez Martinez,[67]
M. J. V. Fernoux,[104] J. Ferrando,[93] A. Ferrari,[167] P. Ferrari,[117,116] R. Ferrari,[73a] D. Ferrere,[56] C. Ferretti,[108]
M. P. Fewell,[1] D. Fiacco,[75a,75b] F. Fiedler,[102] P. Fiedler,[135] S. Filimonov,[39] M. S. Filip,[28b,q] A. Filipčič,[95]
E. K. Filmer,[162a] F. Filthaut,[116] M. C. N. Fiolhais,[133a,133c,r] L. Fiorini,[169] W. C. Fisher,[109] T. Fitschen,[103]
P. M. Fitzhugh,[138] I. Fleck,[147] P. Fleischmann,[108] T. Flick,[177] M. Flores,[34d,s] L. R. Flores Castillo,[64a]
L. Flores Sanz De Acedo,[37] F. M. Follega,[78a,78b] N. Fomin,[33] J. H. Foo,[161] A. Formica,[138] A. C. Forti,[103]
E. Fortin,[37] A. W. Fortman,[18a] L. Foster,[18a] L. Fountas,[9,t] D. Fournier,[66] H. Fox,[93] P. Francavilla,[74a,74b]
S. Francescato,[61] S. Franchellucci,[56] M. Franchini,[24b,24a] S. Franchino,[63a] D. Francis,[37] L. Franco,[48]
L. Franconi,[48] M. Franklin,[61] G. Frattari,[27] Y. Y. Frid,[157] J. Friend,[59] N. Fritzsche,[37] A. Froch,[56]
D. Froidevaux,[37] J. A. Frost,[137] Y. Fu,[109] S. Fuenzalida Garrido,[140g] M. Fujimoto,[151] K. Y. Fung,[64a]
E. Furtado De Simas Filho,[83e] M. Furukawa,[159] M. Fuste Costa,[48] J. Fuster,[169] A. Gaa,[55] A. Gabrielli,[24b,24a]
A. Gabrielli,[161] P. Gadow,[37] G. Gagliardi,[57b,57a] L. G. Gagnon,[18a] S. Gaid,[85b] S. Galantzan,[157] J. Gallagher,[1]
E. J. Gallas,[129] A. L. Gallen,[167] B. J. Gallop,[137] K. K. Gan,[122] S. Ganguly,[159] Y. Gao,[52] A. Garabaglu,[142]
F. M. Garay Walls,[140a,140b] C. García,[169] A. Garcia Alonso,[117] A. G. Garcia Caffaro,[178] J. E. García Navarro,[169]
M. A. Garcia Ruiz,[23b] M. Garcia-Sciveres,[18a] G. L. Gardner,[131] R. W. Gardner,[40] N. Garelli,[164] R. B. Garg,[149]
J. M. Gargan,[33] C. A. Garner,[161] C. M. Garvey,[34a] V. K. Gassmann,[164] G. Gaudio,[73a] V. Gautam,[13] P. Gauzzi,[75a,75b]
J. Gavranovic,[95] I. L. Gavrilenko,[133a] A. Gavrilyuk,[38] C. Gay,[170] G. Gaycken,[126] E. N. Gazis,[10] A. Gekow,[122]
C. Gemme,[57b] M. H. Genest,[60] A. D. Gentry,[115] S. George,[97] T. Geralis,[46] A. A. Gerwin,[123]
P. Gessinger-Befurt,[37] M. E. Geyik,[177] M. Ghani,[173] K. Ghorbanian,[96] A. Ghosal,[147] A. Ghosh,[165] A. Ghosh,[7]
B. Giacobbe,[24b] S. Giagu,[75a,75b] T. Giani,[117] A. Giannini,[62] S. M. Gibson,[97] M. Gignac,[139] D. T. Gil,[87b]
A. K. Gilbert,[87a] B. J. Gilbert,[42] D. Gillberg,[35] G. Gilles,[117] D. M. Gingrich,[2,u] M. P. Giordani,[69a,69c]
P. F. Giraud,[138] G. Giugliarelli,[69a,69c] D. Giugni,[71a] F. Giuli,[76a,76b] I. Gkialas,[9,t] L. K. Gladilin,[38] C. Glasman,[101]
M. Glazewska,[20] R. M. Gleason,[165] G. Glemža,[48] M. Glisic,[126] I. Gnesi,[44b] Y. Go,[30] M. Goblirsch-Kolb,[37]
B. Gocke,[49] D. Godin,[110] B. Gokturk,[22a] S. Goldfarb,[107] T. Golling,[56] M. G. D. Gololo,[34c] A. Golub,[142]
D. Golubkov,[38] J. P. Gombas,[109] A. Gomes,[133a,133b] G. Gomes Da Silva,[147] A. J. Gomez Delegido,[37]
R. Gonçalo,[133a] L. Gonella,[21] A. Gongadze,[155c] F. Gonnella,[21] J. L. Gonski,[149] R. Y. González Andana,[52]
S. González de la Hoz,[169] M. V. Gonzalez Rodrigues,[48] R. Gonzalez Suarez,[167] S. Gonzalez-Sevilla,[56]
L. Goossens,[37] B. Gorini,[37] E. Gorini,[70a,70b] A. Gorišek,[95] T. C. Gosart,[131] A. T. Goshaw,[51] M. I. Gostkin,[39]
S. Goswami,[124] C. A. Gottardo,[37] S. A. Gotz,[111] M. Gouighri,[36b] A. G. Goussiou,[142] N. Govender,[34c]
R. P. Grabarczyk,[129] I. Grabowska-Bold,[87a] K. Graham,[35] E. Gramstad,[128] S. Grancagnolo,[70a,70b] C. M. Grant,[1]
P. M. Gravila,[28f] F. G. Gravili,[70a,70b] H. M. Gray,[18a] M. Greco,[112] M. J. Green,[1] C. Grefe,[25] A. S. Grefsrud,[17]
I. M. Gregor,[48] K. T. Greif,[165] P. Grenier,[149] S. G. Grewe,[112] A. A. Grillo,[139] K. Grimm,[32] S. Grinstein,[13,v]
J.-F. Grivaz,[66] E. Gross,[175] J. Grosse-Knetter,[55] L. Guan,[108] G. Guerrieri,[37] R. Guevara,[128] R. Gugel,[102]
J. A. M. Guhit,[108] A. Guida,[19] E. Guilloton,[173] S. Guindon,[37] F. Guo,[14,114c] J. Guo,[144a] L. Guo,[48] L. Guo,[114b,w]
Y. Guo,[108] Y. Guo,[42] A. Gupta,[49] R. Gupta,[132] S. Gupta,[27] S. Gurbuz,[25] S. S. Gurdasani,[48] G. Gustavino,[75a,75b]
P. Gutierrez,[123] L. F. Gutierrez Zagazeta,[131] M. Gutsche,[50] C. Gutschow,[98] C. Gwenlan,[129] C. B. Gwilliam,[94]
E. S. Haaland,[128] A. Haas,[120] M. Habedank,[59] C. Haber,[18a] H. K. Hadavand,[8] A. Haddad,[41] A. Hadef,[50]
A. I. Hagan,[93] J. J. Hahn,[147] E. H. Haines,[98] M. Haleem,[172] J. Haley,[124] G. D. Hallewell,[104] J. A. Hallford,[48]
K. Hamano,[171] H. Hamdaoui,[167] M. Hamer,[25] S. E. D. Hammoud,[66] E. J. Hampshire,[97] J. Han,[143a] L. Han,[114a]

L. Han,[62] S. Han,[14] K. Hanagaki,[84] M. Hance,[139] D. A. Hangal,[42] H. Hanif,[148] M. D. Hank,[131] J. B. Hansen,[43]
P. H. Hansen,[43] T. Harenberg,[177] S. Harkusha,[179] M. L. Harris,[105] Y. T. Harris,[25] J. Harrison,[13]
N. M. Harrison,[122] P. F. Harrison,[173] M. L. E. Hart,[98] N. M. Hartman,[112] N. M. Hartmann,[111] R. Z. Hasan,[97,137]
Y. Hasegawa,[146] F. Haslbeck,[129] S. Hassan,[17] R. Hauser,[109] M. Haviernik,[136] C. M. Hawkes,[21] R. J. Hawkings,[37]
Y. Hayashi,[159] D. Hayden,[109] C. Hayes,[108] R. L. Hayes,[117] C. P. Hays,[129] J. M. Hays,[96] H. S. Hayward,[94]
M. He,[14,114c] Y. He,[48] Y. He,[98] N. B. Heatley,[96] V. Hedberg,[100] J. Heilman,[35] S. Heim,[48] T. Heim,[18a]
J. J. Heinrich,[126] L. Heinrich,[112] J. Hejbal,[134] M. Helbig,[50] A. Held,[176] S. Hellesund,[17] C. M. Helling,[170]
S. Hellman,[47a,47b] A. M. Henriques Correia,[37] H. Herde,[100] Y. Hernández Jiménez,[151] L. M. Herrmann,[25]
T. Herrmann,[50] G. Herten,[54] R. Hertenberger,[111] L. Hervas,[37] M. E. Hesping,[102] N. P. Hessey,[162a] J. Hessler,[112]
M. Hidaoui,[36b] N. Hidic,[136] E. Hill,[161] T. S. Hillersoy,[17] S. J. Hillier,[21] J. R. Hinds,[109] F. Hinterkeuser,[25]
M. Hirose,[127] S. Hirose,[163] D. Hirschbuehl,[177] T. G. Hitchings,[103] B. Hiti,[95] J. Hobbs,[151] R. Hobincu,[28e]
N. Hod,[175] A. M. Hodges,[168] M. C. Hodgkinson,[145] B. H. Hodkinson,[129] A. Hoecker,[37] D. D. Hofer,[108]
J. Hofer,[169] J. Hofner,[102] M. Holzbock,[37] L. B. A. H. Hommels,[33] V. Homsak,[129] B. P. Honan,[103] J. J. Hong,[68]
T. M. Hong,[132] B. H. Hooberman,[168] W. H. Hopkins,[6] M. C. Hoppesch,[168] Y. Horii,[113] M. E. Horstmann,[112]
S. Hou,[154] M. R. Housenga,[168] J. Howarth,[59] J. Hoya,[6] M. Hrabovsky,[125] T. Hryn'ova,[4] P. J. Hsu,[65]
S.-C. Hsu,[142] T. Hsu,[66] M. Hu,[18a] Q. Hu,[62] S. Huang,[33] X. Huang,[14,114c] Y. Huang,[136] Y. Huang,[114b]
Y. Huang,[14] Z. Huang,[66] Z. Hubacek,[135] F. Huegging,[25] T. B. Huffman,[129] M. Hufnagel Maranha De Faria,[83a]
C. A. Hugli,[48] M. Huhtinen,[37] S. K. Huiberts,[128] R. Hulsken,[106] C. E. Hultquist,[18a] D. L. Humphreys,[105]
N. Huseynov,[12] J. Huston,[109] J. Huth,[61] L. Huth,[48] R. Hyneman,[7] G. Iacobucci,[56] G. Iakovidis,[30]
L. Iconomidou-Fayard,[66] J. P. Iddon,[37] P. Iengo,[72a,72b] Y. Iiyama,[159] T. Iizawa,[159] Y. Ikegami,[84] D. Iliadis,[158]
N. Ilic,[161] H. Imam,[36a] G. Inacio Goncalves,[83d] S. A. Infante Cabanas,[140c] T. Ingebretsen Carlson,[47a,47b]
J. M. Inglis,[96] G. Introzzi,[73a,73b] M. Iodice,[77a] V. Ippolito,[75a,75b] R. K. Irwin,[94] M. Ishino,[159] W. Islam,[176]
C. Issever,[19] S. Istin,[22a,x] K. Itabashi,[127] H. Ito,[174] R. Iuppa,[78a,78b] A. Ivina,[175] V. Izzo,[72a] P. Jacka,[135]
P. Jackson,[1] P. Jain,[48] K. Jakobs,[54] T. Jakoubek,[175] J. Jamieson,[59] W. Jang,[159] S. Jankovych,[136]
M. Javurkova,[105] P. Jawahar,[103] L. Jeanty,[126] J. Jejelava,[155a,y] P. Jenni,[54,z] C. E. Jessiman,[35] C. Jia,[143a]
H. Jia,[170] J. Jia,[151] X. Jia,[112,114c] Z. Jia,[114a] C. Jiang,[52] Q. Jiang,[64b] S. Jiggins,[48] M. Jimenez Ortega,[169]
J. Jimenez Pena,[13] S. Jin,[114a] A. Jinaru,[28b] O. Jinnouchi,[141] P. Johansson,[145] K. A. Johns,[7] J. W. Johnson,[139]
F. A. Jolly,[48] D. M. Jones,[152] E. Jones,[48] K. S. Jones,[8] P. Jones,[33] R. W. L. Jones,[93] T. J. Jones,[94] H. L. Joos,[55]
R. Joshi,[122] J. Jovicevic,[16] X. Ju,[18a] J. J. Junggeburth,[37] T. Junkermann,[63a] A. Juste Rozas,[13,v] M. K. Juzek,[88]
S. Kabana,[140f] A. Kaczmarska,[88] S. A. Kadir,[149] M. Kado,[112] H. Kagan,[122] M. Kagan,[149] A. Kahn,[131]
C. Kahra,[102] T. Kaji,[159] E. Kajomovitz,[156] N. Kakati,[175] N. Kakoty,[13] I. Kalaitzidou,[54] C. W. Kalderon,[30]
S. Kandel,[8] N. J. Kang,[139] D. Kar,[34j] E. Karentzos,[25] K. Karki,[8] O. Karkout,[117] S. N. Karpov,[39]
Z. M. Karpova,[39] V. Kartvelishvili,[93,155b] A. N. Karyukhin,[38] E. Kasimi,[158] J. Katzy,[48] S. Kaur,[35] K. Kawade,[146]
M. P. Kawale,[123] C. Kawamoto,[89] T. Kawamoto,[62] E. F. Kay,[37] S. Kazakos,[109] V. F. Kazanin,[38]
J. M. Keaveney,[34a] R. Keeler,[171] G. V. Kehris,[61] J. S. Keller,[35] J. M. Kelly,[171] J. J. Kempster,[152] O. Kepka,[134]
J. Kerr,[162b] B. P. Kerridge,[137] B. P. Kerševan,[95] L. Keszeghova,[29a] R. A. Khan,[132] A. Khanov,[124]
A. G. Kharlamov,[38] T. Kharlamova,[38] E. E. Khoda,[142] M. Kholodenko,[133a] T. J. Khoo,[19] G. Khoriauli,[172]
Y. Khoulaki,[36a] Y. A. R. Khwaira,[130] B. Kibirige,[34j] D. Kim,[6] D. W. Kim,[18b] Y. K. Kim,[40] N. Kimura,[98]
M. K. Kingston,[55] A. Kirchhoff,[55] C. Kirfel,[25] F. Kirfel,[25] J. Kirk,[137] A. E. Kiryunin,[112] S. Kita,[163]
O. Kivernyk,[25] M. Klassen,[164] C. Klein,[35] L. Klein,[172] M. H. Klein,[45] S. B. Klein,[56] U. Klein,[94]
A. Klimentov,[30] T. Klioutchnikova,[37] P. Kluit,[117] S. Kluth,[112] E. Kneringer,[79] T. M. Knight,[161] A. Knue,[49]
M. Kobel,[50] D. Kobylianskii,[175] S. F. Koch,[129] M. Kocian,[149] P. Kodyš,[136] D. M. Koeck,[126] T. Koffas,[35]
O. Kolay,[50] I. Koletsou,[4] T. Komarek,[88] K. Köneke,[55] A. X. Y. Kong,[1] T. Kono,[121] N. Konstantinidis,[98]
P. Kontaxakis,[56] B. Konya,[100] R. Kopeliansky,[42] S. Koperny,[87a] R. Koppenhofer,[54] K. Korcyl,[88] K. Kordas,[158,aa]
A. Korn,[98] S. Korn,[55] I. Korolkov,[13] N. Korotkova,[38] B. Kortman,[117] O. Kortner,[112] S. Kortner,[112]
W. H. Kostecka,[118] M. Kostov,[29a] V. V. Kostyukhin,[147] A. Kotsokechagia,[37] A. Kotwal,[51] A. Koulouris,[37]
A. Kourkoumeli-Charalampidi,[73a,73b] C. Kourkoumelis,[9] E. Kourlitis,[112] O. Kovanda,[126] R. Kowalewski,[171]
W. Kozanecki,[126] A. S. Kozhin,[38] V. A. Kramarenko,[38] G. Kramberger,[95] P. Kramer,[25] M. W. Krasny,[130]
A. Krasznahorkay,[105] A. C. Kraus,[118] J. W. Kraus,[177] J. A. Kremer,[48] N. B. Krengel,[147] T. Kresse,[50]

L. Kretschmann,[177] J. Kretzschmar,[94] P. Krieger,[161] K. Krizka,[21] K. Kroeninger,[49] H. Kroha,[112] J. Kroll,[134]
J. Kroll,[131] K. S. Krowpman,[109] U. Kruchonak,[39] H. Krüger,[25] N. Krumnack,[81] M. C. Kruse,[51] O. Kuchinskaia,[39]
S. Kuday,[3a] S. Kuehn,[37] R. Kuesters,[54] T. Kuhl,[48] V. Kukhtin,[39] Y. Kulchitsky,[39] S. Kuleshov,[140d,140b] J. Kull,[1]
E. V. Kumar,[111] M. Kumar,[34j] N. Kumari,[48] P. Kumari,[162b] A. Kupco,[134] A. Kupich,[38] O. Kuprash,[54]
H. Kurashige,[86] L. L. Kurchaninov,[162a] O. Kurdysh,[4] A. Kurova,[38] M. Kuze,[141] A. K. Kvam,[105] J. Kvita,[125]
N. G. Kyriacou,[142] M. Laassiri,[30] C. Lacasta,[169] F. Lacava,[75a,75b] H. Lacker,[19] D. Lacour,[130] N. N. Lad,[98]
E. Ladygin,[39] A. Lafarge,[41] B. Laforge,[130] T. Lagouri,[178] F. Z. Lahbabi,[36a] S. Lai,[55,37] W. S. Lai,[98]
I. K. Lakomiec,[55] J. E. Lambert,[171] S. Lammers,[68] W. Lampl,[7] C. Lampoudis,[158,aa] G. Lamprinoudis,[102]
A. N. Lancaster,[118] E. Lançon,[30] U. Landgraf,[54] M. P. J. Landon,[96] V. S. Lang,[54] A. J. Lankford,[165] F. Lanni,[37]
K. Lantzsch,[25] A. Lanza,[73a] M. Lanzac Berrocal,[169] J. F. Laporte,[138] T. Lari,[71a] D. Larsen,[17] L. Larson,[11]
F. Lasagni Manghi,[24b] M. Lassnig,[37] S. D. Lawlor,[145] R. Lazaridou,[165] M. Lazzaroni,[71a,71b] E. T. T. Le,[165]
H. D. M. Le,[109] E. M. Le Boulicaut,[178] L. T. Le Pottier,[18a] B. Leban,[24b,24a] F. Ledroit-Guillon,[60] T. F. Lee,[162b]
L. L. Leeuw,[34c] M. Lefebvre,[171] C. Leggett,[18a] G. Lehmann Miotto,[37] M. Leigh,[56] W. A. Leight,[105]
W. Leinonen,[116] A. Leisos,[158,bb] M. A. L. Leite,[83c] C. E. Leitgeb,[19] R. Leitner,[136] K. J. C. Leney,[45] T. Lenz,[25]
S. Leone,[74a] C. Leonidopoulos,[52] A. Leopold,[150] J. H. Lepage Bourbonnais,[35] R. Les,[109] C. G. Lester,[33]
M. Levchenko,[38] J. Levêque,[4] L. J. Levinson,[175] G. Levrini,[24b,24a] M. P. Lewicki,[88] C. Lewis,[142] D. J. Lewis,[4]
L. Lewitt,[145] A. Li,[30] B. Li,[143a] C. Li,[108] C-Q. Li,[112] H. Li,[143a] H. Li,[103] H. Li,[15] H. Li,[62] H. Li,[143a] J. Li,[144a]
K. Li,[14] L. Li,[144a] R. Li,[178] S. Li,[14,114c] S. Li,[144b,144a] T. Li,[5] X. Li,[106] Y. Li,[14] Z. Li,[159] Z. Li,[14,114c] Z. Li,[62]
S. Liang,[14,114c] Z. Liang,[14] M. Liberatore,[138] B. Liberti,[76a] G. B. Libotte,[83d] K. Lie,[64c] J. Lieber Marin,[83e]
H. Lien,[68] H. Lin,[108] S. F. Lin,[151] L. Linden,[111] R. E. Lindley,[7] J. H. Lindon,[37] J. Ling,[61] E. Lipeles,[131]
A. Lipniacka,[17] A. Lister,[170] J. D. Little,[68] B. Liu,[14] B. X. Liu,[114b] D. Liu,[156] D. Liu,[139] E. H. L. Liu,[21]
J. K. K. Liu,[120] K. Liu,[144b] K. Liu,[144b,144a] M. Liu,[62] M. Y. Liu,[62] P. Liu,[14] Q. Liu,[149] S. Liu,[151] X. Liu,[62]
X. Liu,[143a] Y. Liu,[114b,114c] Y. Liu,[168] Y. L. Liu,[143a] Y. W. Liu,[62] Z. Liu,[66,cc] S. L. Lloyd,[96] E. M. Lobodzinska,[48]
P. Loch,[7] E. Lodhi,[161] K. Lohwasser,[145] E. Loiacono,[48] J. D. Lomas,[21] J. D. Long,[42] I. Longarini,[165]
R. Longo,[168] A. Lopez Solis,[13] N. A. Lopez-canelas,[7] N. Lorenzo Martinez,[4] A. M. Lory,[111] M. Losada,[119a]
G. Löschcke Centeno,[4] X. Lou,[47a,47b] X. Lou,[14,114c] A. Lounis,[66] P. A. Love,[93] M. Lu,[66] S. Lu,[131] Y. J. Lu,[154]
H. J. Lubatti,[142] C. Luci,[75a,75b] F. L. Lucio Alves,[114a] F. Luehring,[68] B. S. Lunday,[131] O. Lundberg,[150]
J. Lunde,[37] N. A. Luongo,[6] M. S. Lutz,[37] A. B. Lux,[26] D. Lynn,[30] R. Lysak,[134] V. Lysenko,[135] E. Lytken,[100]
V. Lyubushkin,[39] T. Lyubushkina,[39] M. M. Lyukova,[151] H. Ma,[30] K. Ma,[62] L. L. Ma,[143a] W. Ma,[62] Y. Ma,[124]
J. C. MacDonald,[102] P. C. Machado De Abreu Farias,[83e] D. Macina,[37] R. Madar,[41] T. Madula,[98] J. Maeda,[86]
T. Maeno,[30] P. T. Mafa,[34c,dd] H. Maguire,[145] M. Maheshwari,[33] V. Maiboroda,[66] A. Maio,[133a,133b,133d] K. Maj,[87a]
O. Majersky,[48] S. Majewski,[126] R. Makhmanazarov,[38] N. Makovec,[66] V. Maksimovic,[16] B. Malaescu,[130]
J. Malamant,[128] Pa. Malecki,[88] V. P. Maleev,[38] F. Malek,[60,ee] M. Mali,[95] D. Malito,[97] U. Mallik,[80,a]
A. Maloizel,[5] S. Maltezos,[10] A. Malvezzi Lopes,[83d] S. Malyukov,[39] J. Mamuzic,[95] G. Mancini,[53] M. N. Mancini,[27]
G. Manco,[73a,73b] J. P. Mandalia,[96] S. S. Mandarry,[152] I. Mandić,[95] L. Manhaes de Andrade Filho,[83a]
I. M. Maniatis,[175] J. Manjarres Ramos,[91] D. C. Mankad,[175] A. Mann,[111] T. Manoussos,[37] M. N. Mantinan,[40]
S. Manzoni,[37] L. Mao,[144a] X. Mapekula,[34c] A. Marantis,[158] R. R. Marcelo Gregorio,[96] G. Marchiori,[5]
C. Marcon,[71a] E. Maricic,[16] M. Marinescu,[48] S. Marium,[48] M. Marjanovic,[123] A. Markhoos,[54] M. Markovitch,[66]
M. K. Maroun,[105] M. C. Marr,[148] G. T. Marsden,[103] E. J. Marshall,[93] Z. Marshall,[18a] S. Marti-Garcia,[169]
J. Martin,[98] T. A. Martin,[137] V. J. Martin,[52] B. Martin dit Latour,[17] L. Martinelli,[75a,75b] M. Martinez,[13,v]
P. Martinez Agullo,[169] V. I. Martinez Outschoorn,[105] P. Martinez Suarez,[37] S. Martin-Haugh,[137]
G. Martinovicova,[136] V. S. Martoiu,[28b] A. C. Martyniuk,[98] A. Marzin,[37] D. Mascione,[78a,78b] L. Masetti,[102]
J. Masik,[103] A. L. Maslennikov,[39] S. L. Mason,[42] P. Massarotti,[72a,72b] P. Mastrandrea,[74a,74b]
A. Mastroberardino,[44b,44a] T. Masubuchi,[127] T. T. Mathew,[126] J. Matousek,[136] D. M. Mattern,[49] K. Mauer,[48]
J. Maurer,[28b] T. Maurin,[59] A. J. Maury,[66] B. Maček,[95] C. Mavungu Tsava,[104] D. A. Maximov,[38] A. E. May,[103]
E. Mayer,[41] R. Mazini,[34j] I. Maznas,[118] S. M. Mazza,[139] E. Mazzeo,[37] J. P. Mc Gowan,[171] S. P. Mc Kee,[108]
C. A. Mc Lean,[6] C. C. McCracken,[170] E. F. McDonald,[107] A. E. McDougall,[117] L. F. Mcelhinney,[93]
J. A. Mcfayden,[152] R. P. McGovern,[131] R. P. Mckenzie,[34j] T. C. Mclachlan,[48] D. J. Mclaughlin,[98]
S. J. McMahon,[137] C. M. Mcpartland,[94] R. A. McPherson,[171,o] S. Mehlhase,[111] A. Mehta,[94] D. Melini,[169]

B. R. Mellado Garcia,[34j] A. H. Melo,[55] F. Meloni,[48] A. M. Mendes Jacques Da Costa,[103] L. Meng,[93] S. Menke,[112]
M. Mentink,[37] E. Meoni,[44b,44a] G. Mercado,[118] S. Merianos,[158] C. Merlassino,[69a,69c] C. Meroni,[71a,71b]
J. Metcalfe,[6] A. S. Mete,[6] E. Meuser,[102] C. Meyer,[68] J-P. Meyer,[138] Y. Miao,[114a] R. P. Middleton,[137]
M. Mihovilovic,[66] L. Mijović,[52] G. Mikenberg,[175] M. Mikestikova,[134] M. Mikuž,[95] H. Mildner,[102] A. Milic,[37]
D. W. Miller,[40] E. H. Miller,[149] A. Milov,[175] D. A. Milstead,[47a,47b] T. Min,[114a] A. A. Minaenko,[38]
I. A. Minashvili,[155b] A. I. Mincer,[120] B. Mindur,[87a] M. Mineev,[39] Y. Mino,[89] L. M. Mir,[13] M. Miralles Lopez,[59]
M. Mironova,[18a] M. Missio,[41] A. Mitra,[173] V. A. Mitsou,[169] Y. Mitsumori,[113] O. Miu,[161] P. S. Miyagawa,[96]
T. Mkrtchyan,[37] M. Mlinarevic,[98] T. Mlinarevic,[98] M. Mlynarikova,[136] L. Mlynarska,[87a] C. Mo,[144a]
S. Mobius,[20] M. H. Mohamed Farook,[115] S. Mohapatra,[42] M. F. Mohd Soberi,[52] S. Mohiuddin,[124]
G. Mokgatitswane,[34j] L. Moleri,[175] U. Molinatti,[129] L. G. Mollier,[20] B. Mondal,[134] S. Mondal,[135] K. Mönig,[48]
E. Monnier,[104] L. Monsonis Romero,[169] J. Montejo Berlingen,[13] A. Montella,[47a,47b] M. Montella,[122]
F. Montereali,[77a,77b] F. Monticelli,[92] S. Monzani,[69a,69c] A. Morancho Tarda,[43] N. Morange,[66]
A. L. Moreira De Carvalho,[48] M. Moreno Llácer,[169] C. Moreno Martinez,[56] J. M. Moreno Perez,[23b] P. Morettini,[57b]
S. Morgenstern,[37] M. Morii,[61] M. Morinaga,[159] M. Moritsu,[90] F. Morodei,[75a,75b] P. Moschovakos,[37] B. Moser,[54]
M. Mosidze,[155b] T. Moskalets,[45] P. Moskvitina,[116] J. Moss,[32] P. Moszkowicz,[87a] A. Moussa,[36d] Y. Moyal,[175]
H. Moyano Gomez,[13] E. J. W. Moyse,[105] T. G. Mroz,[88] S. Muanza,[104] M. Mucha,[25] J. Mueller,[132] R. Müller,[37]
G. A. Mullier,[167] A. J. Mullin,[33] J. J. Mullin,[51] A. C. Mullins,[45] A. E. Mulski,[61] D. P. Mungo,[161] D. Munoz Perez,[169]
F. J. Munoz Sanchez,[103] W. J. Murray,[173,137] M. Muškinja,[95] C. Mwewa,[48] A. G. Myagkov,[38,k] A. J. Myers,[8]
G. Myers,[108] M. Myska,[135] B. P. Nachman,[149] K. Nagai,[129] K. Nagano,[84] R. Nagasaka,[159] J. L. Nagle,[30,ff]
E. Nagy,[104] A. M. Nairz,[37] Y. Nakahama,[84] K. Nakamura,[84] K. Nakkalil,[5] A. Nandi,[63b] H. Nanjo,[127]
E. A. Narayanan,[45] Y. Narukawa,[159] I. Naryshkin,[38] L. Nasella,[71a,71b] S. Nasri,[119b] C. Nass,[25] G. Navarro,[23a]
A. Nayaz,[19] P. Y. Nechaeva,[38] S. Nechaeva,[24b,24a] F. Nechansky,[134] L. Nedic,[129] T. J. Neep,[21] A. Negri,[73a,73b]
M. Negrini,[24b] C. Nellist,[117] C. Nelson,[106] K. Nelson,[108] S. Nemecek,[134] M. Nessi,[37,gg] M. S. Neubauer,[168]
J. Newell,[94] P. R. Newman,[21] Y. W. Y. Ng,[168] B. Ngair,[119a] H. D. N. Nguyen,[110] J. D. Nichols,[123]
R. B. Nickerson,[129] R. Nicolaidou,[138] J. Nielsen,[139] M. Niemeyer,[55] J. Niermann,[37] N. Nikiforou,[37]
V. Nikolaenko,[38,k] I. Nikolic-Audit,[130] P. Nilsson,[30] I. Ninca,[48] G. Ninio,[157] A. Nisati,[75a] R. Nisius,[112]
N. Nitika,[175] E. K. Nkadimeng,[34b] T. Nobe,[159] D. Noll,[149] T. Nommensen,[153] M. B. Norfolk,[145] B. J. Norman,[35]
L. C. Nosler,[18a] M. Noury,[36a] J. Novak,[95] T. Novak,[95] R. Novotny,[135] L. Nozka,[125] K. Ntekas,[165] D. Ntounis,[149]
N. M. J. Nunes De Moura Junior,[83b] J. Ocariz,[130] I. Ochoa,[133a] A. Odella Rodriguez,[13] S. Oerdek,[48,hh]
J. T. Offermann,[40] A. Ogrodnik,[88] A. Oh,[103] C. C. Ohm,[150] H. Oide,[84] M. L. Ojeda,[37] Y. Okumura,[159]
L.F. Oleiro Seabra,[133a] I. Oleksiyuk,[56] G. Oliveira Correa,[13] D. Oliveira Damazio,[30] J. L. Oliver,[165] R. Omar,[68]
Ö. O. Öncel,[54] A. P. O'Neill,[20] A. Onofre,[133a,133e,ii] P. U. E. Onyisi,[11] M. J. Oreglia,[40] D. Orestano,[77a,77b]
R. Orlandini,[77a,77b] R. S. Orr,[161] L. M. Osojnak,[42] Y. Osumi,[113] G. Otero y Garzon,[31] H. Otono,[90] M. Ouchrif,[36d]
F. Ould-Saada,[128] T. Ovsiannikova,[142] M. Owen,[59] R. E. Owen,[137] V. E. Ozcan,[22a] F. Ozturk,[88] N. Ozturk,[8]
S. Ozturk,[82] H. A. Pacey,[129] K. Pachal,[162a] A. Pacheco Pages,[13] C. Padilla Aranda,[13] G. Padovano,[75a,75b]
S. Pagan Griso,[18a] J. Pampel,[25] J. Pan,[178] D. K. Panchal,[11] C. E. Pandini,[60] J. G. Panduro Vazquez,[137]
H. D. Pandya,[1] H. Pang,[138] P. Pani,[48] G. Panizzo,[69a,69c] L. Panwar,[130] L. Paolozzi,[56] S. Parajuli,[168]
A. Paramonov,[6] C. Paraskevopoulos,[53] D. Paredes Hernandez,[64b] S. R. Paredes Saenz,[52] A. Pareti,[73a,73b]
K. R. Park,[42] T. H. Park,[112] F. Parodi,[57b,57a] J. A. Parsons,[42] U. Parzefall,[54] B. Pascual Dias,[41]
L. Pascual Dominguez,[101] E. Pasqualucci,[75a] S. Passaggio,[57b] F. Pastore,[97] P. Patel,[88] U. M. Patel,[51]
J. R. Pater,[103] T. Pauly,[37] F. Pauwels,[136] C. I. Pazos,[164] M. Pedersen,[128] R. Pedro,[133a] S. V. Peleganchuk,[38]
O. Penc,[134] S. Peng,[15] G. D. Penn,[178] K. E. Penski,[111] M. Penzin,[38] B. S. Peralva,[83d] A. P. Pereira Peixoto,[142]
L. Pereira Sanchez,[149] D. V. Perepelitsa,[30,ff] G. Perera,[105] E. Perez Codina,[37] M. Perganti,[10] H. Pernegger,[37]
S. Perrella,[75a,75b] K. Peters,[48] R. F. Y. Peters,[103] B. A. Petersen,[37] T. C. Petersen,[43] E. Petit,[104] V. Petousis,[135]
A. R. Petri,[71a,71b] C. Petridou,[158,aa] T. Petru,[136] M. Pettee,[18a] A. Petukhov,[82] K. Petukhova,[37] R. Pezoa,[140g]
L. Pezzotti,[24b,24a] G. Pezzullo,[178] L. Pfaffenbichler,[37] A. J. Pfleger,[79] T. M. Pham,[176] T. Pham,[107]
P. W. Phillips,[137] G. Piacquadio,[151] E. Pianori,[18a] F. Piazza,[126] R. Piegaia,[31] D. Pietreanu,[28b] A. D. Pilkington,[103]
M. Pinamonti,[69a,69c] J. L. Pinfold,[2] G. Pinheiro Matos,[42] B. C. Pinheiro Pereira,[133a] J. Pinol Bel,[13]
A. E. Pinto Pinoargote,[130] L. Pintucci,[69a,69c] K. M. Piper,[152] A. Pirttikoski,[56] D. A. Pizzi,[35] L. Pizzimento,[64b]

A. Plebani,[33] M.-A. Pleier,[30] V. Pleskot,[136] E. Plotnikova,[39] G. Poddar,[96] R. Poettgen,[100] L. Poggioli,[130]
S. Polacek,[136] G. Polesello,[73a] A. Poley,[148] A. Polini,[24b] C. S. Pollard,[173] Z. B. Pollock,[122] E. Pompa Pacchi,[123]
N. I. Pond,[98] D. Ponomarenko,[68] L. Pontecorvo,[37] S. Popa,[28a] G. A. Popeneciu,[28d] A. Poreba,[37]
D. M. Portillo Quintero,[162a] S. Pospisil,[135] M. A. Postill,[145] P. Postolache,[28c] K. Potamianos,[173] P. A. Potepa,[87a]
I. N. Potrap,[39] C. J. Potter,[33] H. Potti,[153] J. Poveda,[169] M. E. Pozo Astigarraga,[37] R. Pozzi,[37]
A. Prades Ibanez,[76a,76b] S. R. Pradhan,[145] J. Pretel,[171] D. Price,[103] M. Primavera,[70a] L. Primomo,[69a,69c]
M. A. Principe Martin,[101] R. Privara,[125] T. Procter,[87b] M. L. Proffitt,[142] N. Proklova,[131] K. Prokofiev,[64c]
G. Proto,[112] J. Proudfoot,[6] M. Przybycien,[87a] W. W. Przygoda,[87b] A. Psallidas,[46] J. E. Puddefoot,[145]
D. Pudzha,[53] H. I. Purnell,[1] D. Pyatiizbyantseva,[116] J. Qian,[108] R. Qian,[109] D. Qichen,[129] Y. Qin,[13] T. Qiu,[52]
A. Quadt,[55] M. Queitsch-Maitland,[103] G. Quetant,[56] R. P. Quinn,[170] G. Rabanal Bolanos,[61] D. Rafanoharana,[112]
F. Raffaeli,[76a,76b] F. Ragusa,[71a,71b] J. L. Rainbolt,[40] S. Rajagopalan,[30] E. Ramakoti,[39] L. Rambelli,[57b,57a]
I. A. Ramirez-Berend,[35] K. Ran,[108,114c] D. S. Rankin,[131] N. P. Rapheeha,[34j] H. Rasheed,[28b] A. Rastogi,[18a]
S. Rave,[102] S. Ravera,[57b,57a] B. Ravina,[37] I. Ravinovich,[175] M. Raymond,[37] A. L. Read,[128] N. P. Readioff,[145]
D. M. Rebuzzi,[73a,73b] A. S. Reed,[59] K. Reeves,[27] D. Reikher,[37] A. Rej,[49] C. Rembser,[37] H. Ren,[62] M. Renda,[28b]
F. Renner,[48] A. G. Rennie,[59] M. Repik,[56] A. L. Rescia,[57b,57a] S. Resconi,[71a] M. Ressegotti,[57b,57a] S. Rettie,[117]
W. F. Rettie,[35] M. M. Revering,[33] E. Reynolds,[18a] O. L. Rezanova,[39] P. Reznicek,[136] H. Riani,[36d] N. Ribaric,[51]
B. Ricci,[69a,69c] E. Ricci,[78a,78b] R. Richter,[112] S. Richter,[47a,47b] E. Richter-Was,[87b] M. Ridel,[130] S. Ridouani,[36d]
P. Rieck,[120] P. Riedler,[37] E. M. Riefel,[47a,47b] J. O. Rieger,[117] M. Rijssenbeek,[151] M. Rimoldi,[34c] L. Rinaldi,[24b,24a]
P. Rincke,[167,55] G. Ripellino,[167] I. Riu,[13] J. C. Rivera Vergara,[171] F. Rizatdinova,[124] E. Rizvi,[96] B. R. Roberts,[40]
S. S. Roberts,[139] D. Robinson,[33] A. Robson,[59] A. Rocchi,[76a,76b] C. Roda,[74a,74b] F. A. Rodriguez,[118]
S. Rodriguez Bosca,[37] Y. Rodriguez Garcia,[23a] A. M. Rodríguez Vera,[118] S. Roe,[37] J. T. Roemer,[37] O. Røhne,[128]
R. A. Rojas,[37] C. P. A. Roland,[130] A. Romaniouk,[79] E. Romano,[73a,73b] M. Romano,[24b]
A. C. Romero Hernandez,[168] N. Rompotis,[94] L. Roos,[130] S. Rosati,[75a] B. J. Rosser,[40] E. Rossi,[129] E. Rossi,[72a,72b]
L. P. Rossi,[61] L. Rossini,[54] R. Rosten,[122] M. Rotaru,[28b] D. Rousseau,[66] D. Rousso,[48] S. Roy-Garand,[161]
A. Rozanov,[104] Z. M. A. Rozario,[59] Y. Rozen,[156] A. Rubio Jimenez,[169] V. H. Ruelas Rivera,[19] T. A. Ruggeri,[1]
A. Ruggiero,[129] A. Ruiz-Martinez,[169] A. Rummler,[37] G. B. Rupnik Boero,[37] Z. Rurikova,[54] N. A. Rusakovich,[39]
S. Ruscelli,[49] H. L. Russell,[171] G. Russo,[75a,75b] J. P. Rutherfoord,[7] S. Rutherford Colmenares,[33] M. Rybar,[136]
P. Rybczynski,[87a] A. Ryzhov,[45] J. A. Sabater Iglesias,[56] H. F-W. Sadrozinski,[139] F. Safai Tehrani,[75a] S. Saha,[1]
M. Sahinsoy,[82] B. Sahoo,[175] A. Saibel,[169] B. T. Saifuddin,[123] M. Saimpert,[138] G. T. Saito,[83c] M. Saito,[159]
T. Saito,[159] A. Sala,[71a,71b] A. Salnikov,[149] J. Salt,[169] A. Salvador Salas,[157] F. Salvatore,[152] A. Salzburger,[37]
D. Sammel,[54] E. Sampson,[93] D. Sampsonidis,[158,aa] D. Sampsonidou,[126] M. A. A. Samy,[59] J. Sánchez,[169]
V. Sanchez Sebastian,[169] H. Sandaker,[128] C. O. Sander,[48] J. A. Sandesara,[176] M. Sandhoff,[177] C. Sandoval,[23b]
L. Sanfilippo,[63a] D. P. C. Sankey,[137] T. Sano,[89] A. Sansoni,[53] M. Santana Queiroz,[18b] L. Santi,[37] C. Santoni,[41]
H. Santos,[133a,133b] A. Santra,[175] E. Sanzani,[24b,24a] K. A. Saoucha,[85b] J. G. Saraiva,[133a,133d] J. Sardain,[7]
O. Sasaki,[84] K. Sato,[163] C. Sauer,[37] E. Sauvan,[4] P. Savard,[161,u] R. Sawada,[159] C. Sawyer,[137] L. Sawyer,[99]
A. M. Sayed,[27] C. Sbarra,[24b] A. Sbrizzi,[24b,24a] T. Scanlon,[98] J. Schaarschmidt,[142] U. Schäfer,[102]
A. C. Schaffer,[66,45] D. Schaile,[111] R. D. Schamberger,[151] C. Scharf,[19] M. M. Schefer,[20] V. A. Schegelsky,[38]
D. Scheirich,[136] M. Schernau,[140f] C. Scheulen,[56] C. Schiavi,[57b,57a] M. Schioppa,[44b,44a] B. Schlag,[149]
S. Schlenker,[37] J. Schmeing,[177] E. Schmidt,[112] M. A. Schmidt,[177] K. Schmieden,[25] C. Schmitt,[102] N. Schmitt,[102]
S. Schmitt,[48] N. A. Schneider,[111] L. Schoeffel,[138] A. Schoening,[63b] P. G. Scholer,[35] E. Schopf,[147] M. Schott,[25]
S. Schramm,[56] T. Schroer,[56] H-C. Schultz-Coulon,[63a] M. Schumacher,[54] B. A. Schumm,[139] Ph. Schune,[138]
H. R. Schwartz,[7] A. Schwartzman,[149] T. A. Schwarz,[108] Ph. Schwemling,[138] R. Schwienhorst,[109] F. G. Sciacca,[20]
A. Sciandra,[30] G. Sciolla,[27] F. Scuri,[74a] C. D. Sebastiani,[37] K. Sedlaczek,[118] S. C. Seidel,[115] A. Seiden,[139]
B. D. Seidlitz,[42] C. Seitz,[48] J. M. Seixas,[83b] G. Sekhniaidze,[72a] L. Selem,[60] N. Semprini-Cesari,[24b,24a]
A. Semushin,[179] D. Sengupta,[56] V. Senthilkumar,[169] L. Serin,[66] M. Sessa,[72a,72b] H. Severini,[123] F. Sforza,[57b,57a]
A. Sfyrla,[56] Q. Sha,[14] H. Shaddix,[118] A. H. Shah,[33] R. Shaheen,[150] J. D. Shahinian,[131] M. Shamim,[37]
L. Y. Shan,[14] M. Shapiro,[18a] A. Sharma,[37] A. S. Sharma,[170] P. Sharma,[30] P. B. Shatalov,[38] K. Shaw,[152]
S. M. Shaw,[103] Q. Shen,[14] D. J. Sheppard,[148] P. Sherwood,[98] L. Shi,[98] X. Shi,[14] S. Shimizu,[84]
I. P. J. Shipsey,[129,a] S. Shirabe,[90] M. Shiyakova,[39,jj] M. J. Shochet,[40] D. R. Shope,[128] B. Shrestha,[123]

S. Shrestha,[122,kk] I. Shreyber,[39] M. J. Shroff,[171] P. Sicho,[134] A. M. Sickles,[168] E. Sideras Haddad,[34j,166]
A. C. Sidley,[117] A. Sidoti,[24b] F. Siegert,[50] Dj. Sijacki,[16] F. Sili,[62] J. M. Silva,[52] I. Silva Ferreira,[83b]
M. V. Silva Oliveira,[30] S. B. Silverstein,[47a] S. Simion,[66] R. Simoniello,[37] E. L. Simpson,[103] H. Simpson,[152]
L. R. Simpson,[6] S. Simsek,[82] S. Sindhu,[55] P. Sinervo,[161] S. N. Singh,[27] S. Singh,[30] S. Sinha,[48] S. Sinha,[103]
M. Sioli,[24b,24a] K. Sioulas,[9] I. Siral,[37] E. Sitnikova,[48] J. Sjölin,[47a,47b] A. Skaf,[55] E. Skorda,[21] P. Skubic,[123]
M. Slawinska,[88] I. Slazyk,[17] I. Sliusar,[128] V. Smakhtin,[175] B. H. Smart,[137] S. Yu. Smirnov,[140b] Y. Smirnov,[82]
L. N. Smirnova,[38,k] O. Smirnova,[100] A. C. Smith,[42] D. R. Smith,[165] J. L. Smith,[103] M. B. Smith,[35] R. Smith,[149]
H. Smitmanns,[102] M. Smizanska,[93] K. Smolek,[135] P. Smolyanskiy,[135] A. A. Snesarev,[39] H. L. Snoek,[117]
R. M. Snyder,[51] S. Snyder,[30] R. Sobie,[171,o] A. Soffer,[157] C. A. Solans Sanchez,[37] E. Yu. Soldatov,[39]
U. Soldevila,[169] A. A. Solodkov,[34j] S. Solomon,[27] A. Soloshenko,[39] K. Solovieva,[54] O. V. Solovyanov,[41]
P. Sommer,[50] A. Sonay,[13] A. Sopczak,[135] A. L. Sopio,[52] F. Sopkova,[29b] J. D. Sorenson,[115]
I. R. Sotarriva Alvarez,[141] V. Sothilingam,[63a] O. J. Soto Sandoval,[140c,140b] S. Sottocornola,[68] R. Soualah,[85a]
Z. Soumaimi,[36e] D. South,[48] N. Soybelman,[175] S. Spagnolo,[70a,70b] M. Spalla,[112] D. Sperlich,[54] B. Spisso,[72a,72b]
D. P. Spiteri,[59] L. Splendori,[104] M. Spousta,[136] E. J. Staats,[35] R. Stamen,[63a] E. Stanecka,[88]
W. Stanek-Maslouska,[48] M. V. Stange,[50] B. Stanislaus,[18a] M. M. Stanitzki,[48] E. A. Starchenko,[38] G. H. Stark,[139]
J. Stark,[91] P. Staroba,[134] P. Starovoitov,[85b] R. Staszewski,[88] C. Stauch,[111] G. Stavropoulos,[46] A. Stefl,[37]
A. Stein,[102] P. Steinberg,[30] B. Stelzer,[148,162a] H. J. Stelzer,[132] O. Stelzer,[162a] H. Stenzel,[58] T. J. Stevenson,[152]
G. A. Stewart,[37] J. R. Stewart,[124] G. Stoicea,[28b] M. Stolarski,[133a] S. Stonjek,[112] A. Straessner,[50] J. Strandberg,[150]
S. Strandberg,[47a,47b] M. Stratmann,[177] M. Strauss,[123] T. Strebler,[104] P. Strizenec,[29b] R. Ströhmer,[172]
D. M. Strom,[126] R. Stroynowski,[45] A. Strubig,[47a,47b] S. A. Stucci,[30] B. Stugu,[17] J. Stupak,[123] N. A. Styles,[48]
D. Su,[149] S. Su,[62] X. Su,[62] D. Suchy,[29a] A. D. Sudhakar Ponnu,[55] K. Sugizaki,[131] V. V. Sulin,[38]
D. M. S. Sultan,[129] L. Sultanaliyeva,[25] S. Sultansoy,[3b] S. Sun,[176] W. Sun,[14] N. Sur,[100] M. R. Sutton,[152]
M. Svatos,[134] P. N. Swallow,[33] M. Swiatlowski,[162a] A. Swoboda,[37] I. Sykora,[29a] M. Sykora,[136] T. Sykora,[136]
D. Ta,[102] K. Tackmann,[48,hh] A. Taffard,[165] R. Tafirout,[162a] Y. Takubo,[84] M. Talby,[104] A. A. Talyshev,[38]
K. C. Tam,[64b] N. M. Tamir,[157] A. Tanaka,[159] J. Tanaka,[159] R. Tanaka,[66] M. Tanasini,[151] Z. Tao,[170]
S. Tapia Araya,[140g] S. Tapprogge,[102] A. Tarek Abouelfadl Mohamed,[37] S. Tarem,[156] K. Tariq,[14] G. Tarna,[37]
G. F. Tartarelli,[71a] M. J. Tartarin,[91] P. Tas,[136] M. Tasevsky,[134] E. Tassi,[44b,44a] A. C. Tate,[168] Y. Tayalati,[36e,ll]
G. N. Taylor,[107] W. Taylor,[162b] R. J. Taylor Vara,[169] A. S. Tegetmeier,[91] P. Teixeira-Dias,[97] J. J. Teoh,[161]
K. Terashi,[159] J. Terron,[101] S. Terzo,[13] M. Testa,[53] R. J. Teuscher,[161,o] A. Thaler,[79] O. Theiner,[56]
T. Theveneaux-Pelzer,[104] D. W. Thomas,[97] J. P. Thomas,[21] E. A. Thompson,[18a] P. D. Thompson,[21] E. Thomson,[131]
R. E. Thornberry,[45] C. Tian,[62] Y. Tian,[56] V. Tikhomirov,[82] Yu. A. Tikhonov,[39] S. Timoshenko,[38] D. Timoshyn,[136]
E. X. L. Ting,[1] P. Tipton,[178] A. Tishelman-Charny,[30] K. Todome,[141] S. Todorova-Nova,[136] L. Toffolin,[69a,69c]
M. Togawa,[84] J. Tojo,[90] S. Tokár,[29a] O. Toldaiev,[68] G. Tolkachev,[104] E. Tolley,[122] M. Tomoto,[84]
L. Tompkins,[149,mm] E. Torrence,[126] H. Torres,[91] D. I. Torres Arza,[140g] E. Torró Pastor,[169] M. Toscani,[31]
C. Tosciri,[40] M. Tost,[11] D. R. Tovey,[145] T. Trefzger,[172] P. M. Tricarico,[13] A. Tricoli,[30] I. M. Trigger,[162a]
S. Trincaz-Duvoid,[130] D. A. Trischuk,[171] A. Tropina,[39] D. Truncali,[76a,76b] L. Truong,[34c] M. Trzebinski,[88]
A. Trzupek,[88] F. Tsai,[151] M. Tsai,[108] A. Tsiamis,[158] P. V. Tsiareshka,[39] S. Tsigaridas,[162a] A. Tsirigotis,[158,bb]
V. Tsiskaridze,[155a] E. G. Tskhadadze,[155a] Y. Tsujikawa,[89] I. I. Tsukerman,[38] V. Tsulaia,[18a] S. Tsuno,[84]
K. Tsuri,[121] D. Tsybychev,[151] Y. Tu,[64b] A. Tudorache,[28b] V. Tudorache,[28b] S. B. Tuncay,[129] S. Turchikhin,[57b,57a]
I. Turk Cakir,[3a] R. Turra,[71a] T. Turtuvshin,[39,nn] P. M. Tuts,[42] S. Tzamarias,[158,aa] Y. Uematsu,[84] F. Ukegawa,[163]
P. A. Ulloa Poblete,[140c,140b] E. N. Umaka,[30] G. Unal,[37] A. Undrus,[30] G. Unel,[165] J. Urban,[29b] P. Urrejola,[140e]
G. Usai,[8] R. Ushioda,[160] M. Usman,[110] F. Ustuner,[52] Z. Uysal,[82] V. Vacek,[135] B. Vachon,[106] T. Vafeiadis,[37]
A. Vaitkus,[98] C. Valderanis,[111] E. Valdes Santurio,[47a,47b] M. Valente,[37] S. Valentinetti,[24b,24a] A. Valero,[169]
E. Valiente Moreno,[169] A. Vallier,[91] J. A. Valls Ferrer,[169] D. R. Van Arneman,[117] A. Van Der Graaf,[49]
H. Z. Van Der Schyf,[34j] P. Van Gemmeren,[6] M. Van Rijnbach,[37] S. Van Stroud,[98] I. Van Vulpen,[117] P. Vana,[136]
M. Vanadia,[76a,76b] U. M. Vande Voorde,[150] W. Vandelli,[37] E. R. Vandewall,[149] D. Vannicola,[157] L. Vannoli,[53]
R. Vari,[75a] M. Varma,[178] E. W. Varnes,[7] C. Varni,[79] D. Varouchas,[66] L. Varriale,[169] K. E. Varvell,[153]
M. E. Vasile,[28b] L. Vaslin,[84] M. D. Vassilev,[149] A. Vasyukov,[39] L. M. Vaughan,[124] R. Vavricka,[136]
T. Vazquez Schroeder,[13] J. Veatch,[32] V. Vecchio,[103] M. J. Veen,[105] I. Veliscek,[30] I. Velkovska,[95] L. M. Veloce,[161]

F. Veloso,[133a,133c] A. G. Veltman,[52] S. Veneziano,[75a] A. Ventura,[70a,70b] A. Verbytskyi,[112] M. Verducci,[74a,74b]
C. Vergis,[96] M. Verissimo De Araujo,[83b] W. Verkerke,[117] J. C. Vermeulen,[117] C. Vernieri,[149] M. Vessella,[165]
M. C. Vetterli,[148,u] A. Vgenopoulos,[102] N. Viaux Maira,[140g,oo] T. Vickey,[145] O. E. Vickey Boeriu,[145]
G. H. A. Viehhauser,[129] L. Vigani,[63b] M. Vigl,[112] M. Villa,[24b,24a] M. Villaplana Perez,[169] E. M. Villhauer,[40]
E. Vilucchi,[53] M. Vincent,[169] M. G. Vincter,[35] A. Visibile,[117] A. Visive,[117] C. Vittori,[37] I. Vivarelli,[24b,24a]
M. I. Vivas Albornoz,[48] E. Voevodina,[112] F. Vogel,[111] J. C. Voigt,[50] P. Vokac,[135] Yu. Volkotrub,[87b]
L. Vomberg,[25] E. Von Toerne,[25] B. Vormwald,[37] K. Vorobev,[51] M. Vos,[169] K. Voss,[147] M. Vozak,[37]
L. Vozdecky,[123] N. Vranjes,[16] M. Vranjes Milosavljevic,[16] M. Vreeswijk,[117] N. K. Vu,[144b,144a] R. Vuillermet,[37]
O. Vujinovic,[102] I. Vukotic,[40] I. K. Vyas,[35] J. F. Wack,[33] S. Wada,[163] C. Wagner,[149] J. M. Wagner,[18a]
W. Wagner,[177] S. Wahdan,[177] H. Wahlberg,[92] C. H. Waits,[123] J. Walder,[137] R. Walker,[111]
K. Walkingshaw Pass,[59] W. Walkowiak,[147] A. Wall,[131] E. J. Wallin,[100] T. Wamorkar,[18a]
K. Wandall-Christensen,[169] A. Wang,[62] A. Z. Wang,[139] C. Wang,[48] C. Wang,[11] H. Wang,[18a] J. Wang,[64c]
P. Wang,[103] P. Wang,[98] R. Wang,[61] R. Wang,[6] S. M. Wang,[154] S. Wang,[14] T. Wang,[116] T. Wang,[62]
W. T. Wang,[129] W. Wang,[14] X. Wang,[168] X. Wang,[144a] X. Wang,[48] Y. Wang,[151] Y. Wang,[62] Z. Wang,[108]
Z. Wang,[144b] Z. Wang,[108] C. Wanotayaroj,[84] A. Warburton,[106] A. L. Warnerbring,[147] S. Waterhouse,[97]
A. T. Watson,[21] H. Watson,[52] M. F. Watson,[21] E. Watton,[37] G. Watts,[142] B. M. Waugh,[98] J. M. Webb,[54]
C. Weber,[30] H. A. Weber,[19] M. S. Weber,[20] S. M. Weber,[63a] C. Wei,[62] Y. Wei,[54] A. R. Weidberg,[129]
E. J. Weik,[120] J. Weingarten,[49] C. Weiser,[54] C. J. Wells,[48] T. Wenaus,[30] T. Wengler,[37] N. S. Wenke,[112]
N. Wermes,[25] M. Wessels,[63a] A. M. Wharton,[93] A. S. White,[61] A. White,[8] M. J. White,[1] D. Whiteson,[165]
L. Wickremasinghe,[127] W. Wiedenmann,[176] M. Wielers,[137] R. Wierda,[150] C. Wiglesworth,[43] H. G. Wilkens,[37]
J. J. H. Wilkinson,[33] D. M. Williams,[42] H. H. Williams,[131] S. Williams,[33] S. Willocq,[105] B. J. Wilson,[103]
D. J. Wilson,[103] P. J. Windischhofer,[40] F. I. Winkel,[31] F. Winklmeier,[126] B. T. Winter,[54] M. Wittgen,[149]
M. Wobisch,[99] T. Wojtkowski,[60] Z. Wolffs,[117] J. Wollrath,[37] M. W. Wolter,[88] H. Wolters,[133a,133c] M. C. Wong,[139]
E. L. Woodward,[42] S. D. Worm,[48] B. K. Wosiek,[88] K. W. Woźniak,[88] S. Wozniewski,[55] K. Wraight,[59] C. Wu,[161]
C. Wu,[21] J. Wu,[159] M. Wu,[114b] M. Wu,[116] S. L. Wu,[176] S. Wu,[14,pp] X. Wu,[62] Y. Q. Wu,[161] Y. Wu,[62] Z. Wu,[4]
Z. Wu,[114a] J. Wuerzinger,[112] T. R. Wyatt,[103] B. M. Wynne,[52] S. Xella,[43] L. Xia,[114a] M. Xie,[62] A. Xiong,[126]
D. Xu,[14] H. Xu,[62] L. Xu,[62] R. Xu,[131] T. Xu,[108] W. Xu,[114a] Y. Xu,[142] Z. Xu,[52] R. Xue,[132] B. Yabsley,[153]
S. Yacoob,[34a] Y. Yamaguchi,[84] E. Yamashita,[159] H. Yamauchi,[163] T. Yamazaki,[18a] Y. Yamazaki,[86] S. Yan,[59]
Z. Yan,[105] H. J. Yang,[144a,144b] H. T. Yang,[62] S. Yang,[62] T. Yang,[64c] X. Yang,[37] X. Yang,[14] Y. Yang,[159]
Y. Yang,[62] W-M. Yao,[18a] C. L. Yardley,[152] J. Ye,[14] S. Ye,[30] X. Ye,[62] Y. Yeh,[98] I. Yeletskikh,[39] B. Yeo,[18b]
M. R. Yexley,[98] T. P. Yildirim,[129] K. Yorita,[174] C. J. S. Young,[37] C. Young,[149] N. D. Young,[126] Y. Yu,[62]
J. Yuan,[14,114c] M. Yuan,[108] R. Yuan,[144b] L. Yue,[98] M. Zaazoua,[62] B. Zabinski,[88] I. Zahir,[36a] A. Zaio,[57b,57a]
Z. K. Zak,[88] T. Zakareishvili,[169] S. Zambito,[56] J. A. Zamora Saa,[140d] J. Zang,[159] R. Zanzottera,[71a,71b]
O. Zaplatilek,[135] C. Zeitnitz,[177] H. Zeng,[14] D. T. Zenger Jr.,[27] O. Zenin,[38] T. Ženiš,[29a] S. Zenz,[96] D. Zerwas,[66]
M. Zhai,[14,114c] D. F. Zhang,[145] G. Zhang,[14,pp] J. Zhang,[143a] J. Zhang,[6] L. Zhang,[62] L. Zhang,[114a]
P. Zhang,[14,114c] R. Zhang,[114a] S. Zhang,[91] T. Zhang,[159] Y. Zhang,[142] Y. Zhang,[98] Y. Zhang,[62] Y. Zhang,[114a]
Z. Zhang,[18a] Z. Zhang,[143a] Z. Zhang,[66] H. Zhao,[142] T. Zhao,[143a] Y. Zhao,[35] Z. Zhao,[62] Z. Zhao,[62]
A. Zhemchugov,[39] J. Zheng,[114a] K. Zheng,[168] X. Zheng,[62] Z. Zheng,[149] D. Zhong,[168] B. Zhou,[108] B. Zhou,[144b]
H. Zhou,[7] N. Zhou,[144a] Y. Zhou,[15] Y. Zhou,[114a] Y. Zhou,[7] J. Zhu,[108] X. Zhu,[144b] Y. Zhu,[144a] Y. Zhu,[62]
X. Zhuang,[14] K. Zhukov,[68] N. I. Zimine,[39] J. Zinsser,[63b] M. Ziolkowski,[147] L. Živković,[16] A. Zoccoli,[24b,24a]
K. Zoch,[61] A. Zografos,[37] T. G. Zorbas,[145] O. Zormpa,[46] and L. Zwalinski[37]

(ATLAS Collaboration)

[1] *Department of Physics, University of Adelaide, Adelaide, Australia*
[2] *Department of Physics, University of Alberta, Edmonton, Alberta, Canada*
[3a] *Department of Physics, Ankara University, Ankara, Türkiye*
[3b] *Division of Physics, TOBB University of Economics and Technology, Ankara, Türkiye*
[4] *LAPP, Université Savoie Mont Blanc, CNRS/IN2P3, Annecy, France*
[5] *APC, Université Paris Cité, CNRS/IN2P3, Paris, France*

[6]*High Energy Physics Division, Argonne National Laboratory, Argonne, Illinois, USA*
[7]*Department of Physics, University of Arizona, Tucson, Arizona, USA*
[8]*Department of Physics, University of Texas at Arlington, Arlington, Texas, USA*
[9]*Physics Department, National and Kapodistrian University of Athens, Athens, Greece*
[10]*Physics Department, National Technical University of Athens, Zografou, Greece*
[11]*Department of Physics, University of Texas at Austin, Austin, Texas, USA*
[12]*Institute of Physics, Azerbaijan Academy of Sciences, Baku, Azerbaijan*
[13]*Institut de Física d'Altes Energies (IFAE), Barcelona Institute of Science and Technology, Barcelona, Spain*
[14]*Institute of High Energy Physics, Chinese Academy of Sciences, Beijing, China*
[15]*Physics Department, Tsinghua University, Beijing, China*
[16]*Institute of Physics, University of Belgrade, Belgrade, Serbia*
[17]*Department for Physics and Technology, University of Bergen, Bergen, Norway*
[18a]*Physics Division, Lawrence Berkeley National Laboratory, Berkeley, California, USA*
[18b]*University of California, Berkeley, California, USA*
[19]*Institut für Physik, Humboldt Universität zu Berlin, Berlin, Germany*
[20]*Albert Einstein Center for Fundamental Physics and Laboratory for High Energy Physics, University of Bern, Bern, Switzerland*
[21]*School of Physics and Astronomy, University of Birmingham, Birmingham, United Kingdom*
[22a]*Department of Physics, Bogazici University, Istanbul, Türkiye*
[22b]*Department of Physics Engineering, Gaziantep University, Gaziantep, Türkiye*
[22c]*Department of Physics, Istanbul University, Istanbul, Türkiye*
[23a]*Facultad de Ciencias y Centro de Investigaciónes, Universidad Antonio Nariño, Bogotá, Colombia*
[23b]*Departamento de Física, Universidad Nacional de Colombia, Bogotá, Colombia*
[24a]*Dipartimento di Fisica e Astronomia A. Righi, Università di Bologna, Bologna, Italy*
[24b]*INFN Sezione di Bologna, Italy*
[25]*Physikalisches Institut, Universität Bonn, Bonn, Germany*
[26]*Department of Physics, Boston University, Boston, Massachusetts, USA*
[27]*Department of Physics, Brandeis University, Waltham, Massachusetts, USA*
[28a]*Transilvania University of Brasov, Brasov, Romania*
[28b]*Horia Hulubei National Institute of Physics and Nuclear Engineering, Bucharest, Romania*
[28c]*Department of Physics, Alexandru Ioan Cuza University of Iasi, Iasi, Romania*
[28d]*National Institute for Research and Development of Isotopic and Molecular Technologies, Physics Department, Cluj-Napoca, Romania*
[28e]*National University of Science and Technology Politechnica, Bucharest, Romania*
[28f]*West University in Timisoara, Timisoara, Romania*
[28g]*Faculty of Physics, University of Bucharest, Bucharest, Romania*
[29a]*Faculty of Mathematics, Physics and Informatics, Comenius University, Bratislava, Slovak Republic*
[29b]*Department of Subnuclear Physics, Institute of Experimental Physics of the Slovak Academy of Sciences, Kosice, Slovak Republic*
[30]*Physics Department, Brookhaven National Laboratory, Upton, New York, USA*
[31]*Universidad de Buenos Aires, Facultad de Ciencias Exactas y Naturales, Departamento de Física, y CONICET, Instituto de Física de Buenos Aires (IFIBA), Buenos Aires, Argentina*
[32]*California State University, California, USA*
[33]*Cavendish Laboratory, University of Cambridge, Cambridge, United Kingdom*
[34a]*Department of Physics, University of Cape Town, Cape Town, South Africa*
[34b]*iThemba Labs, Western Cape, South Africa*
[34c]*Department of Mechanical Engineering Science, University of Johannesburg, Johannesburg, South Africa*
[34d]*National Institute of Physics, University of the Philippines Diliman (Philippines), Philippines*
[34e]*Department of Physics, Stellenbosch University, Matieland, South Africa*
[34f]*University of KwaZulu-Natal, School of Agriculture and Science, Mathematics, Westville, South Africa*
[34g]*University of South Africa, Department of Physics, Pretoria, South Africa*
[34h]*University of Pretoria, Department of Mechanical and Aeronautical Engineering, Pretoria, South Africa*
[34i]*University of Zululand, KwaDlangezwa, South Africa*
[34j]*School of Physics, University of the Witwatersrand, Johannesburg, South Africa*
[35]*Department of Physics, Carleton University, Ottawa, Ontario, Canada*
[36a]*Faculté des Sciences Ain Chock, Université Hassan II de Casablanca, Morocco*
[36b]*Faculté des Sciences, Université Ibn-Tofail, Kénitra, Morocco*

[36c]*Faculté des Sciences Semlalia, Université Cadi Ayyad, LPHEA-Marrakech, Morocco*
[36d]*LPMR, Faculté des Sciences, Université Mohamed Premier, Oujda, Morocco*
[36e]*Faculté des sciences, Université Mohammed V, Rabat, Morocco*
[36f]*Institute of Applied Physics, Mohammed VI Polytechnic University, Ben Guerir, Morocco*
[37]*CERN, Geneva, Switzerland*
[38]*Affiliated with an institute formerly covered by a cooperation agreement with CERN*
[39]*Affiliated with an international laboratory covered by a cooperation agreement with CERN*
[40]*Enrico Fermi Institute, University of Chicago, Chicago, Illinois, USA*
[41]*LPC, Université Clermont Auvergne, CNRS/IN2P3, Clermont-Ferrand, France*
[42]*Nevis Laboratory, Columbia University, Irvington, New York, USA*
[43]*Niels Bohr Institute, University of Copenhagen, Copenhagen, Denmark*
[44a]*Dipartimento di Fisica, Università della Calabria, Rende, Italy*
[44b]*INFN Gruppo Collegato di Cosenza, Laboratori Nazionali di Frascati, Italy*
[45]*Physics Department, Southern Methodist University, Dallas, Texas, USA*
[46]*National Centre for Scientific Research "Demokritos", Agia Paraskevi, Greece*
[47a]*Department of Physics, Stockholm University, Sweden*
[47b]*Oskar Klein Centre, Stockholm, Sweden*
[48]*Deutsches Elektronen-Synchrotron DESY, Hamburg and Zeuthen, Germany*
[49]*Fakultät Physik, Technische Universität Dortmund, Dortmund, Germany*
[50]*Institut für Kern- und Teilchenphysik, Technische Universität Dresden, Dresden, Germany*
[51]*Department of Physics, Duke University, Durham, North Carolina, USA*
[52]*SUPA—School of Physics and Astronomy, University of Edinburgh, Edinburgh, United Kingdom*
[53]*INFN e Laboratori Nazionali di Frascati, Frascati, Italy*
[54]*Physikalisches Institut, Albert-Ludwigs-Universität Freiburg, Freiburg, Germany*
[55]*II. Physikalisches Institut, Georg-August-Universität Göttingen, Göttingen, Germany*
[56]*Département de Physique Nucléaire et Corpusculaire, Université de Genève, Genève, Switzerland*
[57a]*Dipartimento di Fisica, Università di Genova, Genova, Italy*
[57b]*INFN Sezione di Genova, Italy*
[58]*II. Physikalisches Institut, Justus-Liebig-Universität Giessen, Giessen, Germany*
[59]*SUPA—School of Physics and Astronomy, University of Glasgow, Glasgow, United Kingdom*
[60]*LPSC, Université Grenoble Alpes, CNRS/IN2P3, Grenoble INP, Grenoble, France*
[61]*Laboratory for Particle Physics and Cosmology, Harvard University, Cambridge, Massachusetts, USA*
[62]*Department of Modern Physics and State Key Laboratory of Particle Detection and Electronics,*
University of Science and Technology of China, Hefei, China
[63a]*Kirchhoff-Institut für Physik, Ruprecht-Karls-Universität Heidelberg, Heidelberg, Germany*
[63b]*Physikalisches Institut, Ruprecht-Karls-Universität Heidelberg, Heidelberg, Germany*
[64a]*Department of Physics, Chinese University of Hong Kong, Shatin, N.T., Hong Kong, China*
[64b]*Department of Physics, University of Hong Kong, Hong Kong, China*
[64c]*Department of Physics and Institute for Advanced Study, Hong Kong University of Science*
and Technology, Clear Water Bay, Kowloon, Hong Kong, China
[65]*Department of Physics, National Tsing Hua University, Hsinchu, Taiwan*
[66]*IJCLab, Université Paris-Saclay, CNRS/IN2P3, 91405, Orsay, France*
[67]*Centro Nacional de Microelectrónica (IMB-CNM-CSIC), Barcelona, Spain*
[68]*Department of Physics, Indiana University, Bloomington, Indiana, USA*
[69a]*INFN Gruppo Collegato di Udine, Sezione di Trieste, Udine, Italy*
[69b]*ICTP, Trieste, Italy*
[69c]*Dipartimento Politecnico di Ingegneria e Architettura, Università di Udine, Udine, Italy*
[70a]*INFN Sezione di Lecce, Italy*
[70b]*Dipartimento di Matematica e Fisica, Università del Salento, Lecce, Italy*
[71a]*INFN Sezione di Milano, Italy*
[71b]*Dipartimento di Fisica, Università di Milano, Milano, Italy*
[72a]*INFN Sezione di Napoli, Italy*
[72b]*Dipartimento di Fisica, Università di Napoli, Napoli, Italy*
[73a]*INFN Sezione di Pavia, Italy*
[73b]*Dipartimento di Fisica, Università di Pavia, Pavia, Italy*
[74a]*INFN Sezione di Pisa, Italy*
[74b]*Dipartimento di Fisica E. Fermi, Università di Pisa, Pisa, Italy*
[75a]*INFN Sezione di Roma, Italy*
[75b]*Dipartimento di Fisica, Sapienza Università di Roma, Roma, Italy*
[76a]*INFN Sezione di Roma Tor Vergata, Italy*

[76b]*Dipartimento di Fisica, Università di Roma Tor Vergata, Roma, Italy*
[77a]*INFN Sezione di Roma Tre, Italy*
[77b]*Dipartimento di Matematica e Fisica, Università Roma Tre, Roma, Italy*
[78a]*INFN-TIFPA, Italy*
[78b]*Università degli Studi di Trento, Trento, Italy*
[79]*Universität Innsbruck, Department of Astro and Particle Physics, Innsbruck, Austria*
[80]*University of Iowa, Iowa City, Iowa, USA*
[81]*Department of Physics and Astronomy, Iowa State University, Ames, Iowa, USA*
[82]*Istinye University, Sariyer, Istanbul, Türkiye*
[83a]*Departamento de Engenharia Elétrica, Universidade Federal de Juiz de Fora (UFJF), Juiz de Fora, Brazil*
[83b]*Universidade Federal do Rio De Janeiro COPPE/EE/IF, Rio de Janeiro, Brazil*
[83c]*Instituto de Física, Universidade de São Paulo, São Paulo, Brazil*
[83d]*Rio de Janeiro State University, Rio de Janeiro, Brazil*
[83e]*Federal University of Bahia, Bahia, Brazil*
[84]*KEK, High Energy Accelerator Research Organization, Tsukuba, Japan*
[85a]*Khalifa University of Science and Technology, Abu Dhabi, United Arab Emirates*
[85b]*University of Sharjah, Sharjah, United Arab Emirates*
[86]*Graduate School of Science, Kobe University, Kobe, Japan*
[87a]*AGH University of Krakow, Faculty of Physics and Applied Computer Science, Krakow, Poland*
[87b]*Marian Smoluchowski Institute of Physics, Jagiellonian University, Krakow, Poland*
[88]*Institute of Nuclear Physics Polish Academy of Sciences, Krakow, Poland*
[89]*Faculty of Science, Kyoto University, Kyoto, Japan*
[90]*Research Center for Advanced Particle Physics and Department of Physics, Kyushu University, Fukuoka, Japan*
[91]*L2IT, Université de Toulouse, CNRS/IN2P3, UPS, Toulouse, France*
[92]*Instituto de Física La Plata, Universidad Nacional de La Plata and CONICET, La Plata, Argentina*
[93]*Physics Department, Lancaster University, Lancaster, United Kingdom*
[94]*Oliver Lodge Laboratory, University of Liverpool, Liverpool, United Kingdom*
[95]*Department of Experimental Particle Physics, Jožef Stefan Institute and Department of Physics, University of Ljubljana, Ljubljana, Slovenia*
[96]*Department of Physics and Astronomy, Queen Mary University of London, London, United Kingdom*
[97]*Department of Physics, Royal Holloway University of London, Egham, United Kingdom*
[98]*Department of Physics and Astronomy, University College London, London, United Kingdom*
[99]*Louisiana Tech University, Ruston, Louisiana, USA*
[100]*Fysiska institutionen, Lunds universitet, Lund, Sweden*
[101]*Departamento de Física Teorica C-15 and CIAFF, Universidad Autónoma de Madrid, Madrid, Spain*
[102]*Institut für Physik, Universität Mainz, Mainz, Germany*
[103]*School of Physics and Astronomy, University of Manchester, Manchester, United Kingdom*
[104]*CPPM, Aix-Marseille Université, CNRS/IN2P3, Marseille, France*
[105]*Department of Physics, University of Massachusetts, Amherst, Massachusetts, USA*
[106]*Department of Physics, McGill University, Montreal, Quebec, Canada*
[107]*School of Physics, University of Melbourne, Victoria, Australia*
[108]*Department of Physics, University of Michigan, Ann Arbor, Michigan, USA*
[109]*Department of Physics and Astronomy, Michigan State University, East Lansing, Michigan, USA*
[110]*Group of Particle Physics, University of Montreal, Montreal, Quebec, Canada*
[111]*Fakultät für Physik, Ludwig-Maximilians-Universität München, München, Germany*
[112]*Max-Planck-Institut für Physik (Werner-Heisenberg-Institut), München, Germany*
[113]*Graduate School of Science and Kobayashi-Maskawa Institute, Nagoya University, Nagoya, Japan*
[114a]*Department of Physics, Nanjing University, Nanjing, China*
[114b]*School of Science, Shenzhen Campus of Sun Yat-sen University, China*
[114c]*University of Chinese Academy of Science (UCAS), Beijing, China*
[115]*Department of Physics and Astronomy, University of New Mexico, Albuquerque, New Mexico, USA*
[116]*Institute for Mathematics, Astrophysics and Particle Physics, Radboud University/Nikhef, Nijmegen, Netherlands*
[117]*Nikhef National Institute for Subatomic Physics and University of Amsterdam, Amsterdam, Netherlands*
[118]*Department of Physics, Northern Illinois University, DeKalb, Illinois, USA*
[119a]*New York University Abu Dhabi, Abu Dhabi, United Arab Emirates*
[119b]*United Arab Emirates University, Al Ain, United Arab Emirates*
[120]*Department of Physics, New York University, New York, New York, USA*

[121]*Ochanomizu University, Otsuka, Bunkyo-ku, Tokyo, Japan*
[122]*Ohio State University, Columbus, Ohio, USA*
[123]*Homer L. Dodge Department of Physics and Astronomy, University of Oklahoma, Norman, Oklahoma, USA*
[124]*Department of Physics, Oklahoma State University, Stillwater, Oklahoma, USA*
[125]*Palacký University, Joint Laboratory of Optics, Olomouc, Czech Republic*
[126]*Institute for Fundamental Science, University of Oregon, Eugene, Oregon, USA*
[127]*Graduate School of Science, University of Osaka, Osaka, Japan*
[128]*Department of Physics, University of Oslo, Oslo, Norway*
[129]*Department of Physics, Oxford University, Oxford, United Kingdom*
[130]*LPNHE, Sorbonne Université, Université Paris Cité, CNRS/IN2P3, Paris, France*
[131]*Department of Physics, University of Pennsylvania, Philadelphia, Pennsylvania, USA*
[132]*Department of Physics and Astronomy, University of Pittsburgh, Pittsburgh, Pennsylvania, USA*
[133a]*Laboratório de Instrumentação e Física Experimental de Partículas—LIP, Lisboa, Portugal*
[133b]*Departamento de Física, Faculdade de Ciências, Universidade de Lisboa, Lisboa, Portugal*
[133c]*Departamento de Física, Universidade de Coimbra, Coimbra, Portugal*
[133d]*Centro de Física Nuclear da Universidade de Lisboa, Lisboa, Portugal*
[133e]*Departamento de Física, Escola de Ciências, Universidade do Minho, Braga, Portugal*
[133f]*Departamento de Física Teórica y del Cosmos, Universidad de Granada, Granada (Spain), Spain*
[133g]*Departamento de Física, Instituto Superior Técnico, Universidade de Lisboa, Lisboa, Portugal*
[134]*Institute of Physics of the Czech Academy of Sciences, Prague, Czech Republic*
[135]*Czech Technical University in Prague, Prague, Czech Republic*
[136]*Charles University, Faculty of Mathematics and Physics, Prague, Czech Republic*
[137]*Particle Physics Department, Rutherford Appleton Laboratory, Didcot, United Kingdom*
[138]*IRFU, CEA, Université Paris-Saclay, Gif-sur-Yvette, France*
[139]*Santa Cruz Institute for Particle Physics, University of California Santa Cruz, Santa Cruz, California, USA*
[140a]*Departamento de Física, Pontificia Universidad Católica de Chile, Santiago, Chile*
[140b]*Millennium Institute for Subatomic physics at high energy frontier (SAPHIR), Santiago, Chile*
[140c]*Instituto de Investigación Multidisciplinario en Ciencia y Tecnología, y Departamento de Física, Universidad de La Serena, Chile*
[140d]*Universidad Andres Bello, Department of Physics, Santiago, Chile*
[140e]*Universidad San Sebastian, Recoleta, Chile*
[140f]*Instituto de Alta Investigación, Universidad de Tarapacá, Arica, Chile*
[140g]*Departamento de Física, Universidad Técnica Federico Santa María, Valparaíso, Chile*
[141]*Department of Physics, Institute of Science, Tokyo, Japan*
[142]*Department of Physics, University of Washington, Seattle, Washington, USA*
[143a]*Institute of Frontier and Interdisciplinary Science and Key Laboratory of Particle Physics and Particle Irradiation (MOE), Shandong University, Qingdao, China*
[143b]*School of Physics, Zhengzhou University, China*
[144a]*State Key Laboratory of Dark Matter Physics, School of Physics and Astronomy, Shanghai Jiao Tong University, Key Laboratory for Particle Astrophysics and Cosmology (MOE), SKLPPC, Shanghai, China*
[144b]*State Key Laboratory of Dark Matter Physics, Tsung-Dao Lee Institute, Shanghai Jiao Tong University, Shanghai, China*
[145]*Department of Physics and Astronomy, University of Sheffield, Sheffield, United Kingdom*
[146]*Department of Physics, Shinshu University, Nagano, Japan*
[147]*Department Physik, Universität Siegen, Siegen, Germany*
[148]*Department of Physics, Simon Fraser University, Burnaby, British Columbia, Canada*
[149]*SLAC National Accelerator Laboratory, Stanford, California, USA*
[150]*Department of Physics, Royal Institute of Technology, Stockholm, Sweden*
[151]*Departments of Physics and Astronomy, Stony Brook University, Stony Brook New York, USA*
[152]*Department of Physics and Astronomy, University of Sussex, Brighton, United Kingdom*
[153]*School of Physics, University of Sydney, Sydney, Australia*
[154]*Institute of Physics, Academia Sinica, Taipei, Taiwan*
[155a]*E. Andronikashvili Institute of Physics, Iv. Javakhishvili Tbilisi State University, Tbilisi, Georgia*
[155b]*High Energy Physics Institute, Tbilisi State University, Tbilisi, Georgia*
[155c]*University of Georgia, Tbilisi, Georgia*
[156]*Department of Physics, Technion, Israel Institute of Technology, Haifa, Israel*
[157]*Raymond and Beverly Sackler School of Physics and Astronomy, Tel Aviv University, Tel Aviv, Israel*
[158]*Department of Physics, Aristotle University of Thessaloniki, Thessaloniki, Greece*

[159]*International Center for Elementary Particle Physics and Department of Physics, University of Tokyo, Tokyo, Japan*
[160]*Graduate School of Science and Technology, Tokyo Metropolitan University, Tokyo, Japan*
[161]*Department of Physics, University of Toronto, Toronto, Ontario, Canada*
[162a]*TRIUMF, Vancouver, British Columbia, Canada*
[162b]*Department of Physics and Astronomy, York University, Toronto, Ontario, Canada*
[163]*Division of Physics and Tomonaga Center for the History of the Universe, Faculty of Pure and Applied Sciences, University of Tsukuba, Tsukuba, Japan*
[164]*Department of Physics and Astronomy, Tufts University, Medford, Massachusetts, USA*
[165]*Department of Physics and Astronomy, University of California Irvine, Irvine, California, USA*
[166]*University of West Attica, Athens, Greece*
[167]*Department of Physics and Astronomy, University of Uppsala, Uppsala, Sweden*
[168]*Department of Physics, University of Illinois, Urbana, Illinois, USA*
[169]*Instituto de Física Corpuscular (IFIC), Centro Mixto Universidad de Valencia—CSIC, Valencia, Spain*
[170]*Department of Physics, University of British Columbia, Vancouver, British Columbia, Canada*
[171]*Department of Physics and Astronomy, University of Victoria, Victoria, British Columbia, Canada*
[172]*Fakultät für Physik und Astronomie, Julius-Maximilians-Universität Würzburg, Würzburg, Germany*
[173]*Department of Physics, University of Warwick, Coventry, United Kingdom*
[174]*Waseda University, Tokyo, Japan*
[175]*Department of Particle Physics and Astrophysics, Weizmann Institute of Science, Rehovot, Israel*
[176]*Department of Physics, University of Wisconsin, Madison, Wisconsin, USA*
[177]*Fakultät für Mathematik und Naturwissenschaften, Fachgruppe Physik, Bergische Universität Wuppertal, Wuppertal, Germany*
[178]*Department of Physics, Yale University, New Haven, Connecticut, USA*
[179]*Yerevan Physics Institute, Yerevan, Armenia*

[a] Deceased.
[b] Also at Department of Physics, King's College London, London, United Kingdom.
[c] Also at Institute of Physics, Azerbaijan Academy of Sciences, Baku, Azerbaijan.
[d] Also at Imam Mohammad Ibn Saud Islamic University, Saudi Arabia.
[e] Also at Department of Physics, University of Thessaly, Greece.
[f] Also at An-Najah National University, Nablus, Palestine.
[g] Also at Department of Physics, University of Fribourg, Fribourg, Switzerland.
[h] Also at Department of Physics, Westmont College, Santa Barbara, USA.
[i] Also at Departament de Fisica de la Universitat Autonoma de Barcelona, Barcelona, Spain.
[j] Also at University of Sienna, Italy.
[k] Also at Affiliated with an institute formerly covered by a cooperation agreement with CERN.
[l] Also at The Collaborative Innovation Center of Quantum Matter (CICQM), Beijing, China.
[m] Also at Faculty of Physics, Sofia University, 'St. Kliment Ohridski', Sofia, Bulgaria.
[n] Also at Università di Napoli Parthenope, Napoli, Italy.
[o] Also at Institute of Particle Physics (IPP), Canada.
[p] Also at Department of Physics, Bolu Abant Izzet Baysal University, Bolu, Türkiye.
[q] Also at Faculty of Physics, University of Bucharest, Romania.
[r] Also at Borough of Manhattan Community College, City University of New York, New York, New York, USA.
[s] Also at National Institute of Physics, University of the Philippines Diliman (Philippines), Philippines.
[t] Also at Department of Financial and Management Engineering, University of the Aegean, Chios, Greece.
[u] Also at TRIUMF, Vancouver, British Columbia, Canada.
[v] Also at Institucio Catalana de Recerca i Estudis Avancats, ICREA, Barcelona, Spain.
[w] Also at Henan University, China.
[x] Also at Yeditepe University, Physics Department, Istanbul, Türkiye.
[y] Also at Institute of Theoretical Physics, Ilia State University, Tbilisi, Georgia.
[z] Also at CERN, Geneva, Switzerland.
[aa] Also at Center for Interdisciplinary Research and Innovation (CIRI-AUTH), Thessaloniki, Greece.
[bb] Also at Hellenic Open University, Patras, Greece.
[cc] Also at Department of Modern Physics and State Key Laboratory of Particle Detection and Electronics, University of Science and Technology of China, Hefei, China.
[dd] Also at Department of Mathematical Sciences, University of South Africa, Johannesburg, South Africa.
[ee] Also at Department of Physics, Stellenbosch University, South Africa.

[ff] Also at University of Colorado Boulder, Department of Physics, Colorado, USA.
[gg] Also at Département de Physique Nucléaire et Corpusculaire, Université de Genève, Genève, Switzerland.
[hh] Also at Institut für Experimentalphysik, Universität Hamburg, Hamburg, Germany.
[ii] Also at Centre of Physics of the Universities of Minho and Porto (CF-UM-UP), Portugal.
[jj] Also at Institute for Nuclear Research and Nuclear Energy (INRNE) of the Bulgarian Academy of Sciences, Sofia, Bulgaria.
[kk] Also at Washington College, Chestertown, Maryland, USA.
[ll] Also at Institute of Applied Physics, Mohammed VI Polytechnic University, Ben Guerir, Morocco.
[mm] Also at Department of Physics, Stanford University, Stanford California, USA.
[nn] Also at Institute of Physics and Technology, Mongolian Academy of Sciences, Ulaanbaatar, Mongolia.
[oo] Also at Millennium Institute for Subatomic physics at high energy frontier (SAPHIR), Santiago, Chile.
[pp] Also at University of Chinese Academy of Sciences (UCAS), Beijing, China.